NASA Common Research Model: A History and Future Plans

Melissa B. Rivers[1]
NASA Langley Research Center, Hampton, VA 23681

The NASA Common Research Model (CRM) has enabled many formal and informal international cooperative activities and has enabled aeronautical researchers and engineers in industry, government, and academia to work together across organizational and international borders sharing results on relevant problems for the benefit of all. The NASA Common Research Model (CRM) was conceived in 2007 and its aerodynamic design completed in 2008 responding to needs broadly expressed both within the US and international aeronautics communities for modern/industry-relevant and open/public geometries coupled with advanced experimental data for applied computational fluid dynamic validation studies. This paper provides a brief history of the development of the CRM, along with a summary of wind tunnel model data that has been obtained over the past 10 years. This paper presents data obtained from the NASA Langley National Transonic Facility, the Ames 11-ft Transonic Wind Tunnel and the European Transonic Windtunnel. Sample comparisons are given between the three wind tunnels for lift, drag and pitching moment. Several CRM-derivatives that have been developed are also summarized in this paper.

I. Nomenclature

b	=	*wing span, in.*
c	=	*wing mean aerodynamic chord, in.*
C_D	=	*drag coefficient*
C_L	=	*lift coefficient*
C_m	=	*pitching moment coefficient referenced to 0.25 of the wing mean aerodynamic chord*
M_∞	=	*freestream Mach number*
q_∞	=	*dynamic pressure, psf*
Re_c	=	*Reynolds number based on mean aerodynamic chord*
S	=	*model reference area, ft^2*
α	=	*angle of attack, deg*
η	=	*fraction of wing semi-span*
Λ	=	*leading edge sweep angle*
σ	=	*standard deviation*
θ	=	*wing twist, deg*

II. Introduction

The NASA Common Research Model (CRM) has enabled many formal and informal international cooperative activities and has enabled aeronautical researchers and engineers in industry, government, and academia to work together across organizational and international borders sharing results on relevant problems for the benefit of all. The creation of the CRM was motived by needs broadly expressed both within the US and international aeronautics communities for modern/industry-relevant and open/public geometries coupled with advanced experimental data (e.g. skin friction and off-body flow field data for example) suitable for applied computational fluid dynamic (CFD) validation studies. One specific need was for a contemporary commercial transport geometry expressed by the AIAA Applied Aerodynamics Technical Committee-sponsored international Drag Prediction Workshop (DPW) community after completing DPW-I, II, and III between 2001-06. In 2007, NASA's Subsonic Fixed Wing (SFW) Project within the Fundamental Aeronautics Program (FAP) took the lead and developed the idea of a modern, industry-relevant yet

[1] Senior Research Engineer, Configuration Aerodynamics Branch, Mail Stop 267, AIAA Associate Fellow.

non-proprietary geometry and through its Aerodynamics Technical Working Group (ATWG) led a group of US aerodynamics leaders from industry and government to define the goals and characteristics of the transport configuration that became known as the NASA CRM. Boeing then took the lead for the detailed aerodynamic design of the CRM configuration; the geometry definition was a critical item because it strikes the difficult balance between being both modern/industry-relevant (Mach 0.85/supercritical, so people and organizations care) and open/public (non-proprietary, so the worldwide community can participate). The detailed aerodynamic design was vetted with the SFW ATWG and other experts before freezing the design in 2008 and reported by Vassberg [**1,2**] et. al. Once the aerodynamic design was complete, wind tunnel model hardware was next.

NASA's SFW Project led the hardware design, fabrication, and initial testing of the NASA CRM to meet the broad objectives to provide open/public data for CFD validation studies and to provide an anchor for experimental measurements and correction methods between facilities. NASA's initial commitment was to complete two tests that would provide data for the international DPW-IV (2009, blind calculations) [**3**], along with an offer to entertain collaboration opportunities with additional organizations for further tests of the CRM to add to the public database. The CRM was initially tested in the National Transonic Facility (NTF) at the NASA Langley Research Center in 2010 to provide a baseline data set for this geometry [**4**]. This initial test obtained force and moment, surface pressure, model deformation, and surface flow visualization data that were used for CFD validation for DPW-IV. The model then was tested at the Ames 11-Foot Transonic Wind Tunnel Facility (11-ft) in 2010 [**5**]. The next stop for the CRM was again the NTF in 2013 to provide test to test repeatability information adding to the wind tunnel and to add to the growing CRM experimental database. The CRM database continued to provide test cases for DPW-V (2012) [**6**] and DPW-VI (2016) [**7**]. In 2014, the model made its first international journey under a NASA/DLR collaborative agreement and was tested at the European Transonic Windtunnel (ETW) as part of an EU initiative, and added more information to the experimental database [**8**]. And now, the CRM is scheduled to be tested in the NTF in 2019 to provide more repeatability data and to once again add further to the CRM experimental database. To facilitate the dissemination of the acquired data, a website was set up to provide a place where people from all over the world can retrieve information specifically related to their needs [**9**]. The purpose of this paper is to summarize the data acquired to date with the original NASA CRM hardware in preparation for the next entry of the CRM.

Many organizations worldwide have embraced the CRM geometry for both computational and experimental research. Variations of the original CRM have been fabricated and tested in facilities all over the world. These variations will be discussed later in the paper. Further CRM-based collaborations and use of the configuration are wide and varied – far beyond the initial expectations in 2007 when the concept was conceived and beyond the scope of this paper; a future paper is envisioned to capture and summarize the broader use and benefit of the NASA CRM configuration.

III. Design and Fabrication

This section provides additional detail on aerodynamic design and NASA CRM wind tunnel model hardware design and fabrication complementing the more general discussion above. The CRM aerodynamics design consists of a contemporary supercritical transonic wing and a fuselage that is representative of a wide-body commercial transport aircraft. The CRM was designed for a cruise Mach number of $M_\infty = 0.85$ with a design lift coefficient of $C_L = 0.5$. A sketch of the CRM with reference quantities listed is shown in **Fig. 1**. The aspect ratio is 9.0, the leading-edge sweep angle (Λ) is 35 deg, the wing reference area (S) is 3.01 ft^2, the wingspan (b) is 62.46 inches, and the mean aerodynamic chord (c) is 7.45 inches. The model moment reference center is located 35.8 inches aft of the fuselage nose and 2.04 inches below the fuselage centerline. The nacelles are simple, flow-through nacelles. The model was designed to measure pressures on both the left and right wings using 291 pressure orifices located in nine spanwise wing stations (η = 0.131, 0.201, 0.283, 0.397, 0.502, 0.603, 0.727, 0.846, and 0.950) and on the left-hand nacelle by six orifices at six radial stations (η = 30˚, 90˚, 150˚, 210˚, 270˚, and 330˚). Two wing root bending gages and two Kulite pressure transducers were also installed in the wings. Five different configurations were designed: the wing/body (WB) alone, wing/body/nacelle/pylon (WBNP), wing/body/tail = 0˚ (WBT0), wing/body/tail = +2˚ (WBT+2), and wing/body/tail = -2˚ (WBT-2).

The fabrication of the CRM model was performed by Microcraft in Tullahoma, TN. The contract was awarded to Microcraft in July of 2008 and fabricated out of cryogenically acceptable steel, Vascomax C250. The model hardware was delivered to NASA in December 2009. The model was then prepared for its first test in the NTF.

IV. Experimental Tests

A. National Transonic Facility

1. First entry, 2010

The first test of the CRM was performed at the NTF **[10, 11]** at the NASA Langley Research Center in January of 2010. The NTF is a unique national facility that enables testing of aircraft configurations at conditions ranging from subsonic to low supersonic speeds at Reynolds numbers up to full-scale flight values. The NTF is a conventional, closed circuit, continuous-flow, fan-driven, pressurized wind tunnel (**Fig. 2**) capable of operating in either dry air at warm temperatures or nitrogen from warm to cryogenic temperatures.

This investigation, designated NTF 197, provided force and moment, surface pressure, model deformation, surface flow visualization, wing bending moment and Kulite data. Testing was conducted at 5, 19.8 and 30 million Reynolds number based on the mean aerodynamic chord. To isolate static aeroelastic effects, the 19.8 million Reynolds number data were collected at two different q_∞ levels. The data were collected at temperatures ranging from -250ºF up to 120ºF and Mach numbers ranging from 0.7 to 0.87. All Reynolds number values presented in this paper are based on mean aerodynamic chord and all data presented in this paper were obtained at the design Mach number of 0.85.

Data were generally obtained over an angle-of-attack range from -3° to +12° at 5 million Reynolds number and an angle-of-attack range from -3° to +6° at 19.8 and 30 million Reynolds numbers. The reduced angle-of-attack range at the higher Reynolds number was required such that critical model stress levels would not be exceeded. Flow angularity measurements were made and upflow corrections ranging from 0.092° to 0.173° were applied to the final NTF data. Wall corrections accounting for model blockage, wake blockage, tunnel buoyancy, and lift interference were also applied. Testing on the WBNP, WBT+2, and WBT-2 configurations was conducted at a Reynolds number of 5 million only. However, data were obtained at all three Reynolds numbers for both the WB and WBT0 configurations. The model is mounted in the wind tunnel using a blade sting arrangement as shown in **Fig. 3**.

Another important set of data obtained in this investigation was model deformation measurements. Since an effective correlation of computational and experimental data will be directly tied to how well the computational and experimental model geometries match one another, it is important to obtain an accurate definition of the model geometry as tested under aerodynamic loads. In order to obtain this information a video model deformation measurement technique **[12]** has been developed and employed multiple times at the NTF. This system was used in this initial investigation to obtain wing deflection and twist measurements due to aerodynamic loading.

During this test, continuous pitch sweep runs were conducted to acquire Kulite pressure transducer data and wing root bending gage data. The model was pitched at a rate of 0.1 degree/second. The data from the wing root bending gages and Kulites were analyzed by Balakrishna and Acheson **[13]**.

Further tunnel details and facility information are provided in **Ref. [14]** and more detailed information on this NTF test are provided in **Ref. [4]**.

2. Second NTF entry, 2013

The third test of the CRM, designated as NTF 215, was performed in the NTF in July of 2013. The purpose of this test was to obtain data to demonstrate improvements in the NTF and to provide long term test to test repeatability. Testing was limited to the WB, WBT0, and WBNP configurations during this test. This investigation also provided force and moment, surface pressure and model deformation data for comparison to the first entry in the NTF. Testing was again conducted at 5, 19.8 and 30 million Reynolds number and at two different q_∞ levels – a high and a low q_∞ condition for the Re_c = 19.8 million cases to isolate aeroelastic effects. The data were also collected at temperatures ranging from -250ºF up to 120ºF and Mach numbers ranging from 0.7 to 0.87. All data presented in this paper for this test were obtained at a freestream Mach number of 0.85, the design Mach number. The rest of the test setup was identical to the first test of the CRM in the NTF. A limited set of NTF 215 data is presented herein; comparisons and observations documenting the results of the improvements will be provided in a future paper.

B. Ames 11-ft Transonic Wind Tunnel

The second test of the CRM took place at the Ames 11-ft wind tunnel in March of 2010 and was designated Test 216. The Ames 11-ft tunnel is a closed circuit, variable-pressure, continuous operation wind tunnel (**Fig. 4**). References [**15]** and [**16]** provide more detailed information about the facility. The purpose of this test was twofold: first, to provide tunnel to tunnel comparison data at low Reynolds number and second, to leverage a wider range of advanced measurement techniques available in a noncryogenic tunnel.

This investigation acquired force and moment, surface pressure, and surface flow visualization data for comparison to the NTF data, as well as limited pressure sensitive paint (PSP) **[17]** and Fringe Imaging Skin Friction (FISF) technique data **[18]**. Testing was conducted at a chord Reynolds number of 5 million. The data were collected at

temperatures of approximately 100ºF. Data were obtained at freestream Mach numbers ranging from 0.7 to 0.87 but only the 0.85 data are presented in this paper. Data were generally obtained over an angle-of-attack range from -3° to +12° at 5 million chord Reynolds number. Wall corrections accounting for model blockage, wake blockage, tunnel buoyancy, and lift interference were also applied. A picture of the CRM mounted in the 11-ft wind tunnel is shown in **Fig. 5.** More detailed information on this test in the 11-ft tunnel is given in **Ref. [5]**.

C. European Transonic Facility

The fourth test of the CRM was conducted in the European Transonic Wind Tunnel (ETW) in February 2014. The ETW has a smaller test section and lower maximum pressure, but is otherwise very similar to the NTF as both are pressurized cryogenic, closed circuit, continuous-flow, fan-driven wind tunnels (**Fig. 6)**. Further details about the ETW and its operation can be found at www.etw.de. The focus of this test was to improve unsteady testing capabilities for exploring limits of the flight envelope, specifically unsteady wake interference effects between the wake of an aircraft wing and the horizontal tail plane as part of the European ESWIRP project (European Strategic Wind Tunnels Improved Research Potential) **[19].**

During this investigation, force and moment, surface pressure, wing deformation and PIV data were obtained. Although data were acquired at 12 different Mach numbers ranging from 0.25 to 0.87, the majority of the test focused on $M_\infty = 0.7$ and the model design Mach number of 0.85. Only the $M_\infty = 0.85$ data are presented herein. To cover the relevant Reynolds numbers of 5, 19.8 and 30 million, the tunnel temperature was varied between 84°F (302K) and -249°F (117K) combined with corresponding pressures between 29psia (200 kPa) and 44psia (300 kPa). A photo of the model installed in the ETW is shown in **Fig. 7.** Further details on this investigation are given in **Ref. [8]**.

V. Results

A. NTF 197

Since the first NTF test was the inaugural test of the CRM, the database from this test is extensive. The first goal was to assess the nacelle/pylon incremental effects for this configuration. **Fig. 8** shows a representative plot of the nacelle/pylon effects. This figure indicates that at a Mach number of 0.85, the drag increases, the lift decreases and the pitching moment increases at $C_L = 0.5$ when a nacelle/pylon is added to the wing/body configuration, as expected.

The next goal of this test was to determine aeroelastic effect on this new geometry. A typical plot of the aeroelastic effects is shown in **Fig. 9.** This figure shows the aeroelastic effects on the WBT0 configuration at $M_\infty = 0.85$ and $Re_c = 19.8$ million. An increase in q_∞ gives a higher C_D value, a lower C_L and a higher pitching moment for this configuration, which does not follow expected trends. An increase in dynamic pressure is expected to cause a decrease in C_D instead of an increase. The cause for this anomaly is still being researched.

Determining tail effects was also a goal during NTF 197. Three different horizontal tail settings were tested on the WB configuration: tail = -2º, tail = 0º and tail = +2º. **Fig. 10** shows an example of the tail effects, specifically for the $M_\infty = 0.85$ condition. At this condition, there is a decrease in drag, increase in lift and a decrease in pitching moment when going from a -2º to a +2º tail setting, as expected.

The most significant goal of the initial investigation in the NTF was to establish a database for Reynolds numbers from 5 million up to 30 million such that an assessment of Reynolds number effects could be made. Data were obtained at 5, 19.8 and 30 million Reynolds number at three different Mach numbers for the WB and WBT0 configurations. **Figures 11 and 12** show examples of the Reynolds number effects for the WB and WBT0 configurations, respectively, at Mach 0.85. The lift coefficients at this Mach number for the WB configuration show an increase in lift with an increase in Reynolds number. The WBT0 configuration also shows an increase in lift with an increase in Reynolds number except for the low q_∞, 19.8 million case. A reduction in drag is noted for both configurations from 5 to 30 million Reynolds number but the WBT0 19.8 million, low q_∞ cases does not fit this trend, since the 19.8 million low q_∞ data seems to fall right on top of the 30 million data. In addition, as Reynolds number is increased there is a decrease in pitching moment for the WB configuration. For the WBT0 configuration, little to no Reynolds number effect is seen for the pitching moment except for the low q_∞, 19.8 million Reynolds number case, which shows a much smaller pitching moment than the other Reynolds numbers. This may be explained by the fact that at the lower q_∞ the wing does not twist as much which leads to a higher local angle outboard. This means more lift and more nose down for the lower q_∞ compared to the higher q_∞.

Another goal of the initial test of the CRM was to evaluate model twist. **Figures 13–16** show example twist plots from the test. These plots show the aeroelastic twist vs. C_L at Mach 0.85 for the 5 positions on the wing measured during the test. These four figures are for the WBT0 configuration at $Re_c = 5$ million-low q_∞, 19.8 million-low q_∞,

19.8 million-high q_∞, and 30 million-high q_∞. The higher Reynolds number data (**Figures 14-16**) have a distinct break close to $C_L = 0.6$, consistent with separation near the tip.

During NTF 197, multiple repeat runs were obtained for all five of the configurations tested (WB, WBPN WBT0, WBT+2, and WBT-2) to provide an assessment of data repeatability. Sample repeatability data for this test are presented in **Figs. 17 and 18**. Delta coefficient data are presented versus angle of attack for each configuration at each condition. The delta coefficient data presented represent the difference between the coefficient value measured and the average value of the coefficient at that particular angle of attack. These delta coefficient, or residual, data show the level of variation in the repeat runs. The solid lines shown on each plot indicate the 2-sigma limits based on all the data across the angle-of-attack range. Thus, it is shown that most all of the residual data fall within the 2-sigma limits, which is true for most of the data from this test [**4**].

B. Ames 11-ft Test 216

When the CRM was taken to Ames 11-ft for testing, many of the same goals were in place. Determining the effects of adding a nacelle/pylon to the configuration was one goal. **Figure 19** shows an example of these effects at $M_\infty = 0.85$ for both the Ames 11-ft and LaRC NTF tests. This figure shows that the drag increases, the lift lowers and the pitching moment increases at $C_L = 0.5$ and $M_\infty = 0.85$ with the addition of a nacelle/pylon in both wind tunnel tests. The slopes are the same for lift, drag and pitching moment with negligible differences in the values of pitching moment between the wind tunnel tests. At $M_\infty = 0.85$, there is approximately an eight drag count difference and a difference of 0.01 in lift for both the WB and WBPN configurations between the wind tunnel tests.

Another goal of the Ames 11-ft test was to determine the horizontal tail effects for the CRM model. Three different tail settings were tested at both wind tunnels on the WB configuration: tail = -2º, tail = +2º and tail = 0º. All of these cases were run at a chord Reynolds number of 5 million. **Figure 20** shows the tail effects for a Mach number of 0.85. This figure shows that for the $C_L = 0.5$ and $M_\infty = 0.85$ condition, there is again a decrease in drag, an increase in lift and a decrease in pitching moment when going from a -2º to a +2º tail setting at Ames 11-ft just like at NTF, with negligible difference between the wind tunnel pitching moment actual values. The drag values between the Ames 11-ft and NTF tests give a difference of approximately eight drag counts for the WBT-2 setting, a difference of approximately six drag counts for the WBT0 and 11 drag counts for the WBT+2 setting. The difference in lift is approximately 0.004 for both the WBT+2 and WBT0 settings and approximately 0.006 for the WBT-2 setting.

The data repeatability for the Ames 11-ft test was checked in the same manner as at NTF, i.e., within each series of runs, three runs were obtained at the given Mach number. Each of these three runs were always separated by at least one run at a different test condition. This resulted in three repeat runs for all of the configurations at the conditions tested. Sample repeatability data resulting from these runs at $M_\infty = 0.85$ is presented in **Fig. 21** which shows that most all of the data are within the 2-sigma limits. This is typical of all of the data from this test [**5**].

C. NTF Test 215

One goal of the second test of the CRM in the NTF was to provide long-term repeatability data for the CRM database. With this being the case, the main focus while analyzing the data was on test-to-test repeatability. **Figures 22-26** show the test-to-test comparisons for the WB configuration at $M_\infty = 0.85$ and Reynolds number varying from 5 up to 30 million and WBT0 configurations at $M_\infty = 0.85$ and Reynolds number varying from 5 up to 19.8 million.

Delta coefficient data are presented versus angle of attack for each configuration at each condition shown. The delta coefficient data presented represent the difference between the coefficient value measured and the average value of the coefficient at that particular angle of attack. These delta coefficient, or residual, data show the level of variation in the runs between the tests. The solid lines shown on each plot indicate the 2-sigma limits based on all the data across the angle-of-attack range. These figures show that most of the data fall within the 2-sigma limits which indicates very good repeatability between the tests.

D. ETW test

While comparison with the NTF tests was not a primary goal of the test of the CRM in the ETW, the data acquired did enable these comparisons. **Figure 27** shows the comparison between NTF 197, NTF 215 and ETW at $M_\infty = 0.85$ and $Re_c = 5$ million. This figure shows that at this condition, the NTF lift data is lower than the ETW data and the NTF drag data is ~ three drag counts lower than the ETW data. Finally, the NTF pitching moment is higher than the ETW data at the given condition.

Figure 28 shows comparisons for the $Re_c = 19.8$ million case at the low q_∞ value. At $M_\infty = 0.85$ and design point of $C_L = 0.5$, the between-test NTF drag data indicates almost no difference between NTF 197 and NTF 215, but is four counts higher than the ETW data. Off of this design point the drag differences vary slightly over the polar. The NTF

197 and NTF 215 lift difference is negligible and is lower than ETW. For the pitching moment, the NTF197 data is 0.001 more nose up than the ETW data but the NTF 215 data is 0.003 higher than the ETW data.

The results for the $Re_c = 19.8$ million case at a high q_∞ value case are given in **Fig. 29**. At $M_\infty = 0.85$, the difference in drag data between the NTF tests is negligible but is seven drag counts higher than the ETW data. The lift data difference between the two NTF tests is negligible but is 0.026 lower than the ETW lift data. The pitching moment indicates a change in slope above the design point of $C_L = 0.5$ between the two NTF tests. A better agreement is seen between NTF 215 and ETW below the design point of $C_L = 0.5$ and a better agreement between the two NTF tests above this design point. The cause of the change in slope between the two NTF test data is unknown.

At a flight Reynolds number of $Re_c = 30$ million and $M_\infty = 0.85$, shown in **Fig. 30**, the NTF drag data is nine counts higher than the ETW data, the NTF lift data is lower than ETW and the pitching moment data is higher than ETW. More details on the comparison between the ETW and NTF 197 tests is provided in **Ref. [8]**.

VI. CRM Derivatives

Variations of the original CRM have been fabricated and tested in facilities all over the world. The Japan Aerospace Exploration Agency (JAXA) built and tested an 80% scaled version of the NASA CRM hardware. This model (**Fig. 31**) was tested in the JAXA 2m x 2m transonic wind tunnel in 2012 [**20**]. The data from this test was compared to the data from the first NTF entry. These comparisons showed differences in drag and pitching moment due to a lower Reynolds number set point in the JAXA tunnel due to tunnel limitations (data not shown in this paper). Further investigation looking into Reynolds number corrections and corrections for model deformation has been conducted that provide some possible reasons for the lack of agreement between the two wind tunnels[**21**].

Another derivative of the CRM fabricated by the Office National d'Etudes et de Recherches Aerospactiales (ONERA), the French Aeronautics and Space Research Center, is called the Large Reference Model (LRM) and was tested in their S1MA wind tunnel. This model was a 220% scaled version of the NASA CRM hardware. This model was the first (and only one thus far) to include a vertical tail **[22**]. A picture of the LRM installed in the S1MA wind tunnel is shown in **Fig. 32**.

In 2016 the port wing of the NASA CRM hardware was borrowed by the National Research Council (NRC) in Canada for an experimental test program in the NRC 5-Foot Trisonic Wind Tunnel semispan test facility. The existing wing was mounted to a newly fabricated half-model fuselage. The configuration of the wind tunnel semispan facility required the model be installed inverted as shown in **Fig. 33**. The week-long test program provided valuable information that the NRC will be able to utilize in the development of semispan test capabilities at the NRC 5-Foot Trisonic Wind Tunnel. The comparison between the data from this NRC test program and the first NTF test data show similar lift and moment characteristics when measured on the semispan configuration (data not shown in this paper). Incremental effects of the nacelle/pylon can be assessed with similar accuracy as in a fullspan test but the absolute drag coefficients obtained with the semispan setup are significantly biased and require additional analysis to establish a methodology to correct [**23**].

Another derivative of the CRM geometry is the Common Research Model-High Lift (CRM-HL). This model was developed in an effort to obtain the required high lift performance using active flow control (AFC) on simple-hinged flaps while reducing the cruise drag associated with the external mechanisms on slotted flaps of a generic modern transport aircraft [**24-26**]. This 10% scale high-lift configuration of the CRM was designed for testing at the NASA Langley Research Center 14- by 22-Foot Subsonic Wind Tunnel in 2018, and is ongoing as of the writing of this paper. A depiction of the CRM-HL model is shown in **Fig. 34**.

More recently, a semispan wing based on the CRM geometry was designed for Natural Laminar Flow (NLF) on the upper surface and tested in the NTF in 2018, designated CRM-NLF. This new wing was designed to experimentally validate a new NLF technology called Crossflow Attenuated Natural Laminar Flow (CATNLF). This technology enables significant extents of NLF on wings with sweep and Reynolds number typical of transports by using geometry shaping to obtain surface pressures that delay boundary layer transition due to crossflow. A picture of this new wing mounted in the NTF is shown in **Fig. 35** and more information about the experiment is given in **Ref. [27]**.

Acknowledgments

The author would like to gratefully acknowledge the efforts of the NASA and ETW teams throughout all phases of these experimental investigations and the AIAA Drag Prediction Workshop Committee for their support during the design and fabrication of the CRM. The LaRC NTF, Ames 11-ft and ETW staff are recognized for their efforts in effectively obtaining all desired experimental data. Within NASA, work was funded by various projects over the years, including the Subsonic Fixed Wing Project under the Fundamental Aeronautics Program, the Aerosciences

Evaluation and Test Capability (AETC) project and the Advanced Air Transport Technology Project within the Advanced Air Vehicles Program.

References

[1] Vassberg, J. C., DeHaan, M. A., Rivers, S. M., and Wahls, R. A., "Development of a Common Research Model for Applied CFD validation studies." AIAA Paper 2008-6919, 26th AIAA Applied Aerodynamics Conference, Honolulu, HI, August 2008.

[2] Vassberg, J. C., DeHaan, M. A., Rivers, S. M., and Wahls, R. A., "Retrospective on the Common Research Model for Computational Fluid Dynamics Validation Studies,", Journal of Aircraft 2018, Vol. 55, No. 4 (2018), pp. 1325-1337.

[3] Vassberg, J. C., et al., "Summary of the Fourth AIAA CFD Drag Prediction Workshop," AIAA Paper 2010-4547, 28th AIAA Applied Aerodynamics Conference, Chicago, IL, 2010.

[4] Rivers, Melissa B. and Dittberner, Ashley, "Experimental Investigation of the NASA Common Research Model," AIAA Paper 2010-4218, 28th AIAA Applied Aerodynamics Conference, Chicago, IL, June 2010.

[5] Rivers, Melissa B. and Dittberner, Ashley, "Experimental Investigations of the NASA Common Research Model in the NASA Langley National Transonic Facility and NASA Ames 11-Ft Transonic Wind Tunnel (Invited)," AIAA Paper 2011-1126, 49th AIAA Aerospace Sciences Meeting, Orlando, FL, January 2011.

[6] Levy, David W., et al., "Summary of Data from the Fifth AIAA CFD Drag Prediction Workshop,", AIAA Paper 2013-0046, 51st AIAA Aerospace Sciences Meeting, Grapevine, TX, January 2013.

[7] Tinoco, E. N., et al., "Summary Data from the Sixth AIAA CFD Drag Prediction Workshop: CRM Cases 2 to 5," AIAA Paper 2017-1208, 55th AIAA Aerospace Sciences Meeting, Grapevine, TX, January 2017.

[8] Rivers, Melissa B., Quest, Juergen, and Rudnik, Ralf, "Comparison of the NASA Common Research Model European Transonic Wind Tunnel Test Data to NASA Test Data," AIAA Paper 2015-1093, 53rd AIAA Aerospace Sciences Meeting, January 2015.

[9] NASA Common Research Model [online database], NASA, https://commonresearchmodel.larc.nasa.gov/ [retrieved 1 November 2018].

[10] Gloss, B. B., "Current Status and Some Future Test Directions for the US National Transonic Facility. Wind Tunnels and Wind Tunnel Test Techniques," Royal Aeronautical Society , 1992, pp. 3.1-3.7.

[11] Wahls, R. A., "The National Transonic Facility: A Research Retrospective (Invited)," AIAA Paper 2001-0754, 39th AIAA Aerospace Sciences Meeting and Exhibit, Reno, Nevada, January 2001.

[12] Burner, A. W. and Liu, T., "Videogrammetric Model Deformation Measurement Technique," Journal of Aircraft, Vol. 38, No. 4, July-August 2001, pp. 745-754.

[13] Balakrishna, S. and Acheson, Michael J., "Analysis of NASA Common Research Model Dynamic Data," AIAA Paper 2011-1127, 49th AIAA Aerospace Sciences Meeting, Orlando, FL, January 2011.

[14] Fuller, D. E., "Guide for Users of the National Transonic Facility," *NASA TM-83124*, 1981.

[15] Kmak, F., "Modernization and Activation of the NASA Ames 11-by-11-Foot Transonic Wind Tunnel," AIAA Paper 2000-2680, 21st Aerodynamic Measurement Technology and Ground Testing Conference, June 2000.

[16] Amaya, M.A. and Murthy, S.V., "Flow Quality Measurements in the NASA Ames Upgraded 11-by-11-Foot Transonic Wind Tunnel (invited Paper)," AIAA Paper 2000-2681, 21st Aerodynamic Measurement Technology and Ground Testing Conference. June 2000.

[17] Bell, James H., "Pressure-Sensitive Paint Measurements on the NASA Common Research Model in the NASA 11-ft Transonic Wind Tunnel," AIAA Paper 2011-1128, 49th AIAA Aerospace Sciences Meeting, Orlando, FL, January 2011.

[18] Zilliac, et. al., "A Comparison of the Measured and Computed Skin Friction Distribution on the Common Research Model," AIAA Paper 2011-1129, 49th AIAA Aerospace Sciences Meeting, Orlando, FL, January 2011.

[19] Lutz, Thorsten, et. al., "Going for Experimental and Numberical Unsteady Wake Analyses Combined with Wall Interference Assesment by Using the NASA CRM Model in ETW," AIAA Paper 2013-0871, 51st AIAA Aerospace Sciences Meeting, Grapevine, TX, January 2013.

[20] Ueno, M., Kohzai, T., Koga, S., Kato, H. Nakakita, K., and Sudani, N., "80% Scaled NASA Common Research Model Wind Tunnel Test of JAXA at Relatively Low Reynolds Number," AIAA Paper 2013-0493, 51st AIAA Aerospace Sciences Meeting, Grapevine, TX, January 2013.

[21] Kohzai, M., Ueno, M., Koga, S., and Sudani, N., "Wall and Support Interference Corrections of NASA Common Research Model Wind Tunnel Tests in JAXA," AIAA Paper 2013-0963, 51st AIAA Aerospace Sciences Meeting, Grapevine, TX, January 2013.

[22] Cartieri, A., Hue, D., Chanzy, Q., and Atinault, O., "Experimental Investigations on the Common Research Model at ONERA-S1MA – Comparison with DPW Numerical Results," AIAA Paper 2017-0964, 55th AIAA Aerospace Sciences Meeting, Grapevine, TX, January 2017.

[23] Broughton, Cabot A., Benmeddour, Ali, Mebarki, Youssef, and Rivers, Melissa B., "Experimental Investigations of the NASA Common Research Semispan Model in the NRC 5-Foot Trisonic Wind Tunnel," AIAA Paper 2018-4285, 2018 Aerodynamic Measurement Technology and Ground Testing Conference, Atlanta, GA, June 2108.

[24] Lacy, Doug S. and Sclafani, Anthony J., "Development of the High Lift Common Research Model (HL-CRM): A Representative High Lift Configuration for Transonic Transports," AIAA Paper 2016-0308, 54th AIAA Aerospace Sciences Meeting, San Diego, CA January 2016.

[25] Hartwich, Peter M., Shmilovich, Arvin, Lacy, Douglas S., Dickey, Eric D., Sclafani, Anthony J., Sundaram, P., and Yadlin, Yoram, "Refined AFC-Enabled High-Lift System Integration Study," NASA/CR-2016-219170, 2016.

[26] Lin, John C., Melton, Latunia P., Viken, Sally A., Andino, Marlyn Y., Koklu, Mehti, Hannon, Judith A. and Vatsa, Veer N., "High Lift Common Research Model for Wind Tunnel Testing: An Active Flow Control Perspective," AIAA Paper 2017-0319, 55th AIAA Aerospace Sciences Meeting, Grapevine, TX, January 2017.

[27] Lynde, M., Campbell, R., Rivers, M., Viken, S., Chan, D., Watkins, A. N., and Goodliff, S., "Preliminary Results from an Experimental Assessment of a Natural Laminar Flow Design Method," AIAA SciTech Forum, San Diego, CA, January 2019 (to be published).

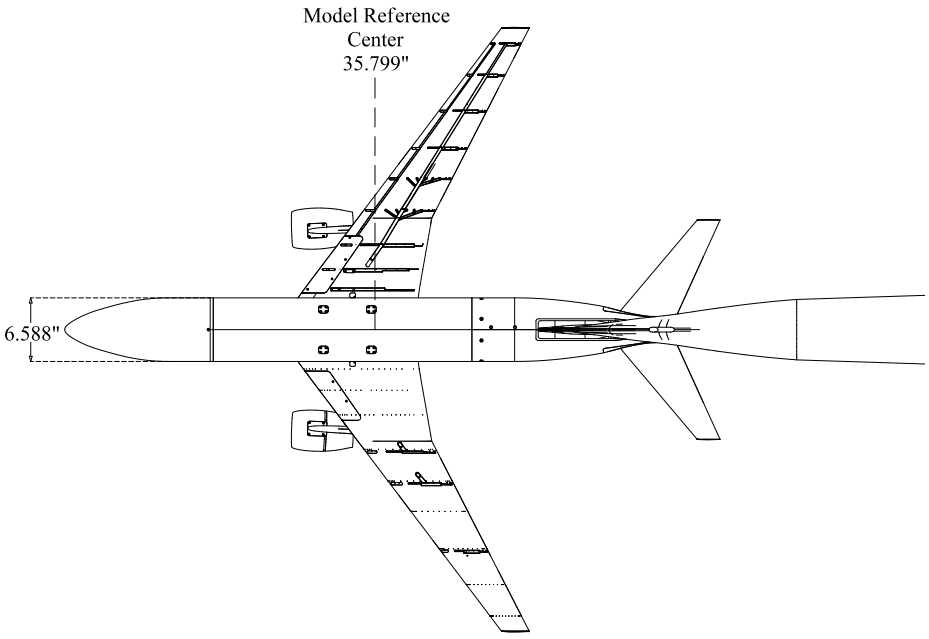

a)Top View

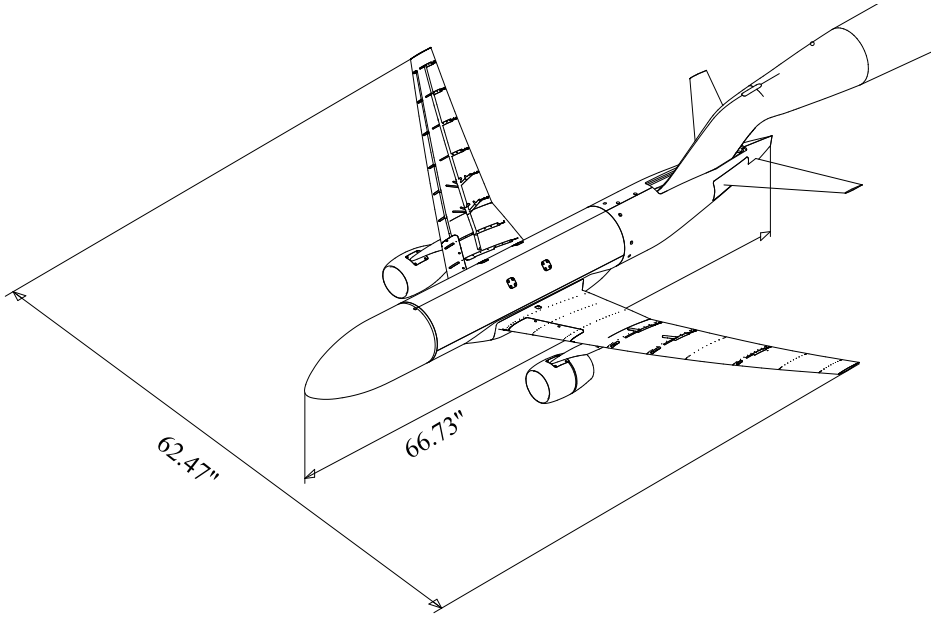

b) Isometric View

Fig. 1. Sketch of the Common Research Model with reference quantities.

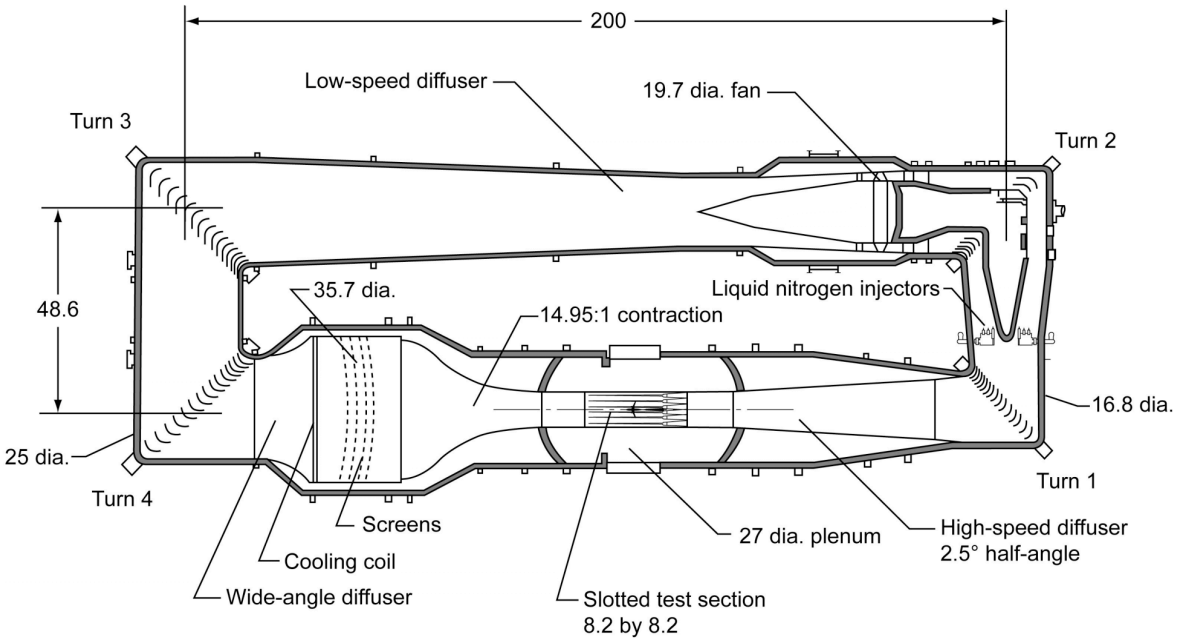

Fig. 2. Sketch of the National Transonic Facility tunnel circuit. Linear dimensions are given in feet.

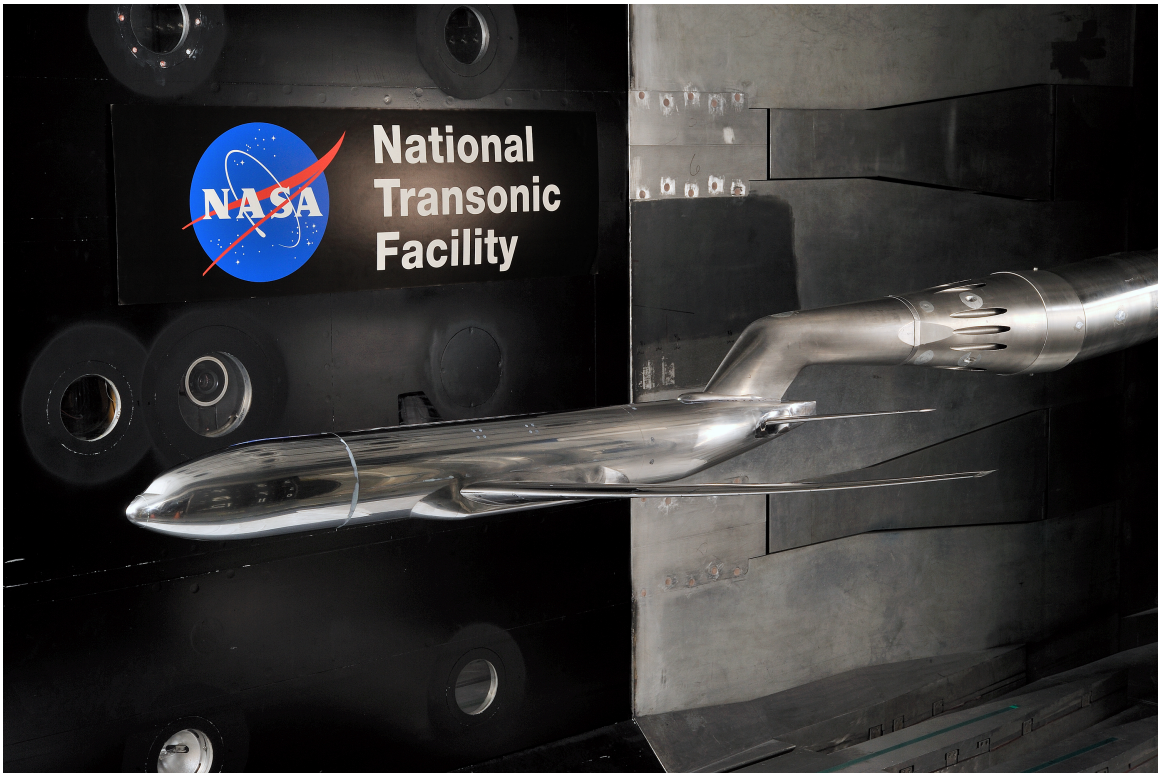

Fig. 3. Photo of the Common Research Model in the National Transonic Facility.

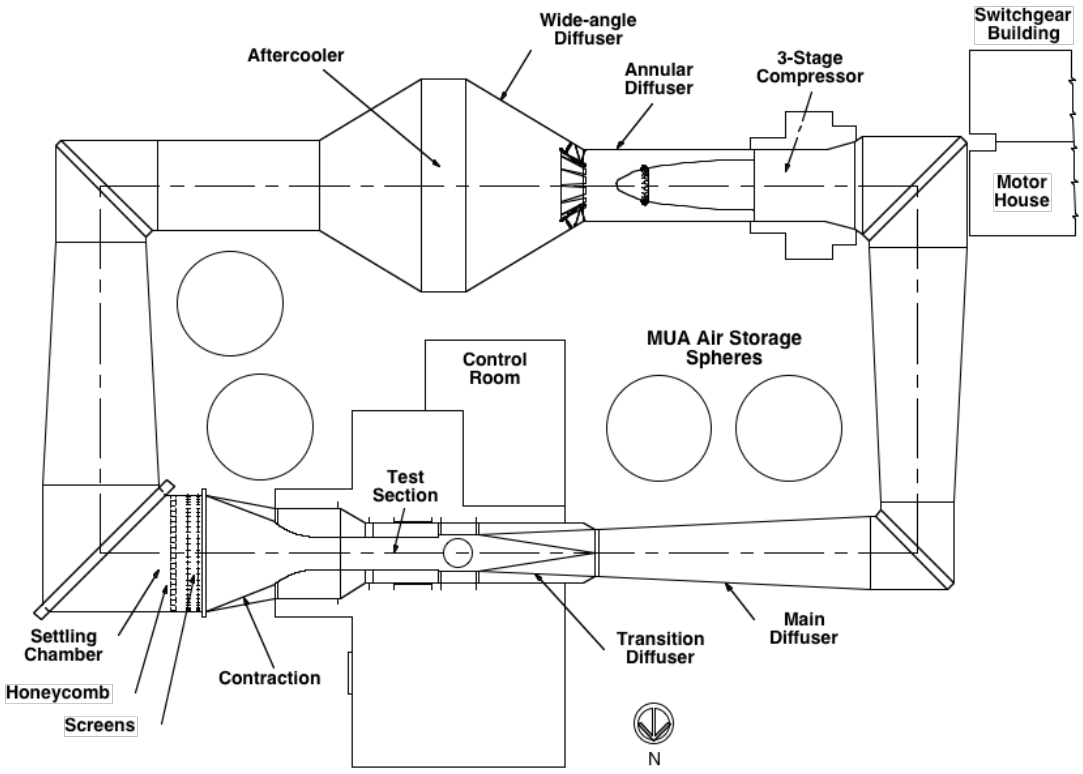

Fig. 4. Sketch of the Ames 11-Foot Transonic Wind Tunnel Facility.

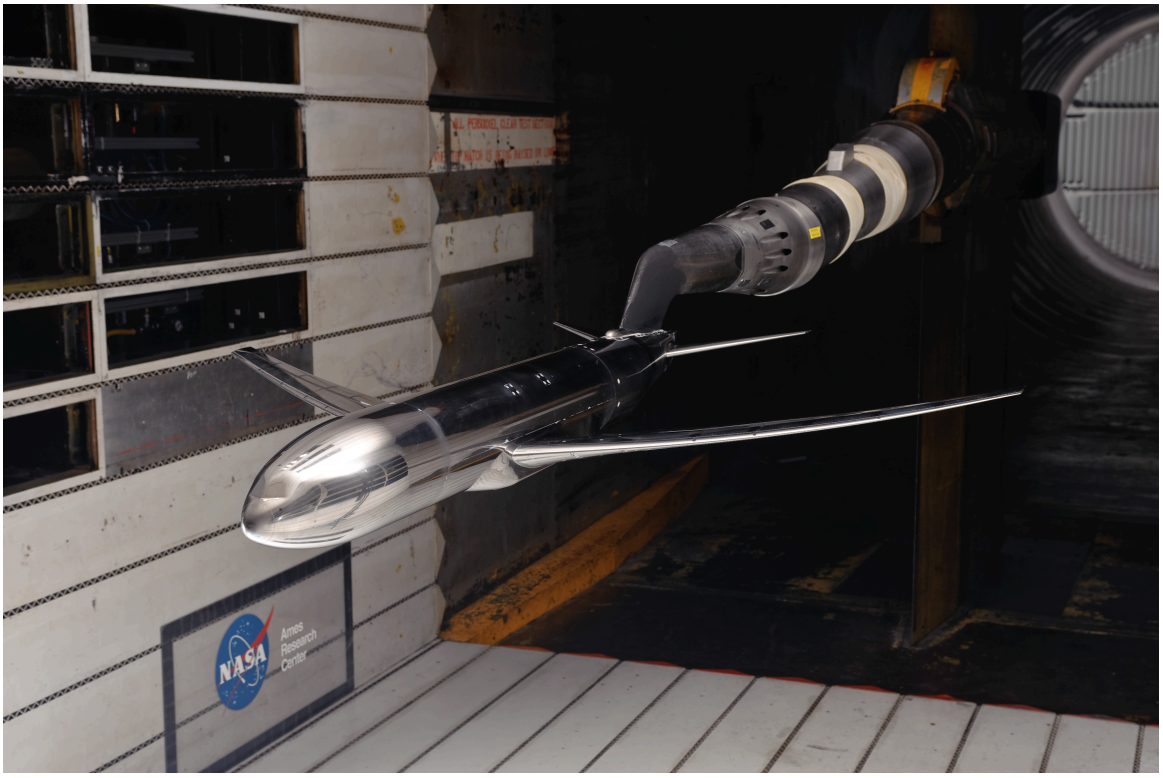

Fig. 5. Photo of the NASA Common Research Model in the Ames 11-Foot Transonic Wind Tunnel Facility.

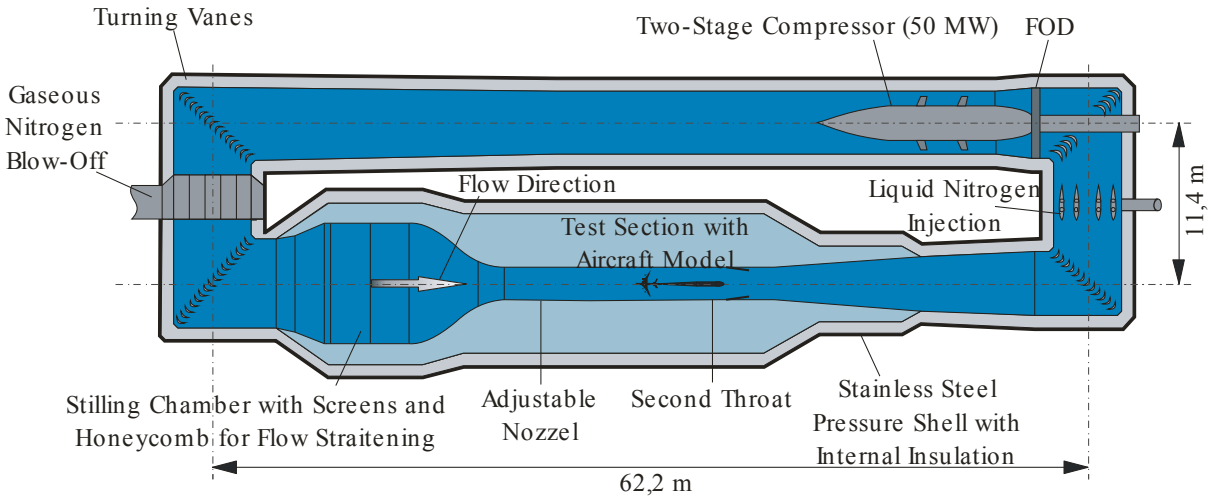

Fig. 6. Sketch of the European Transonic Wind Tunnel.

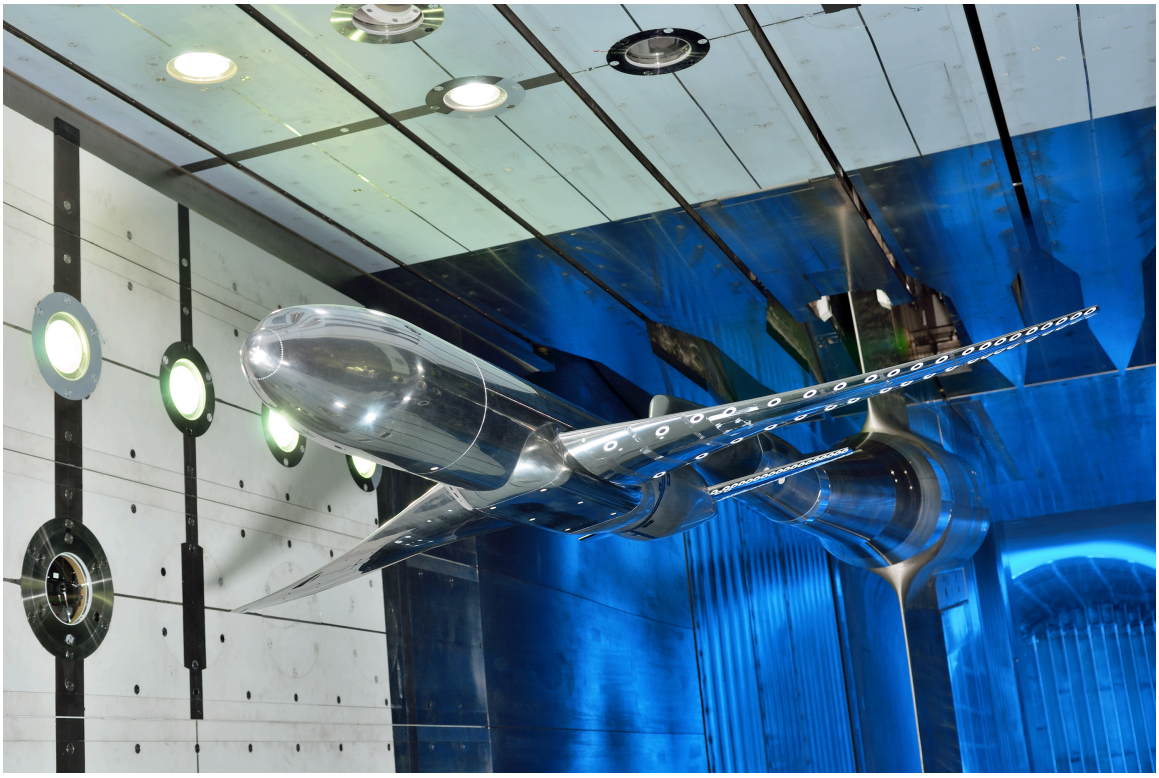

Fig. 7. Photo of the NASA Common Research Model in the European Transonic Windtunnel.

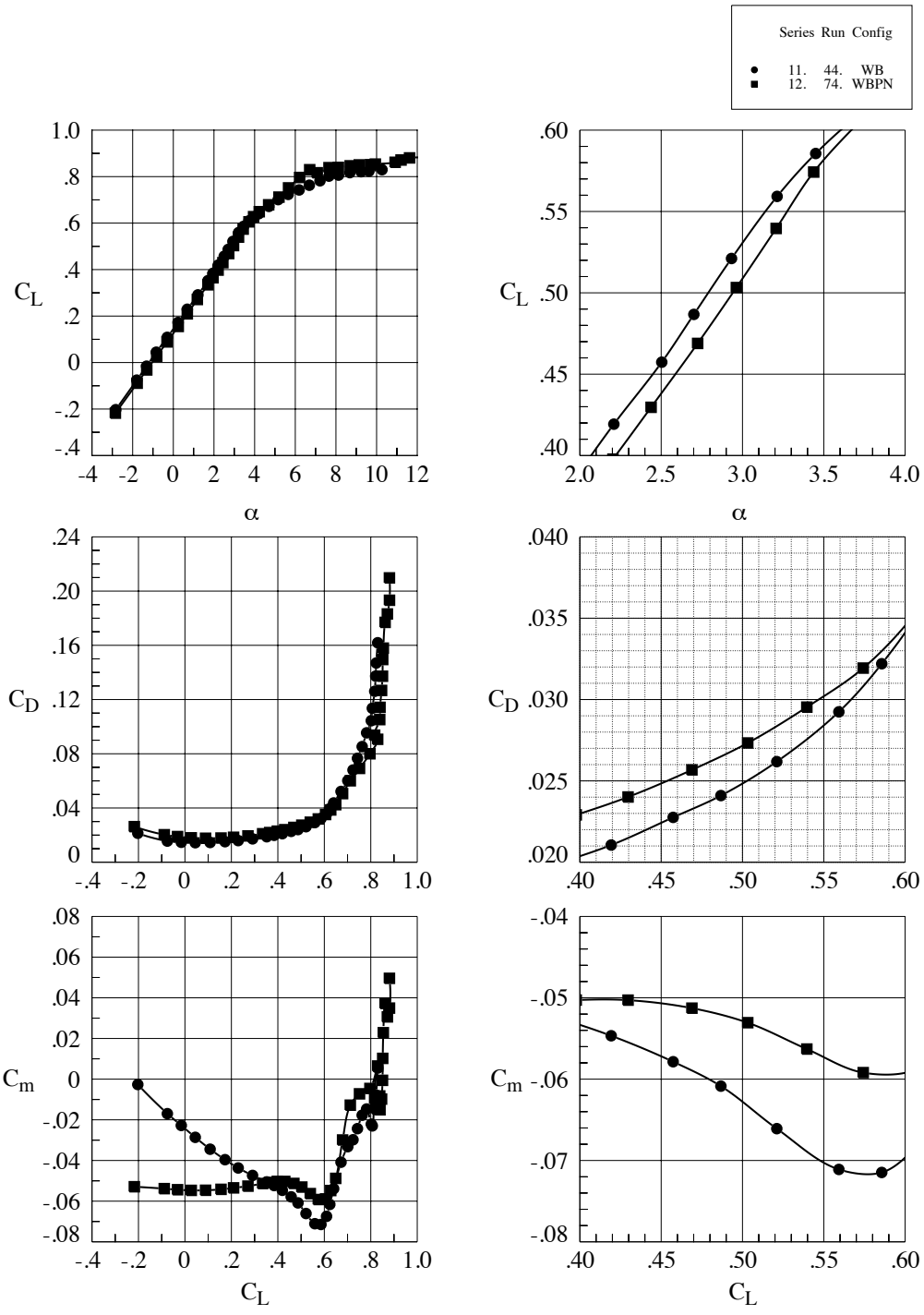

Fig. 8. NTF 197, nacelle/pylon effects, $M_\infty = 0.85$, $Re_c = 5$ million.

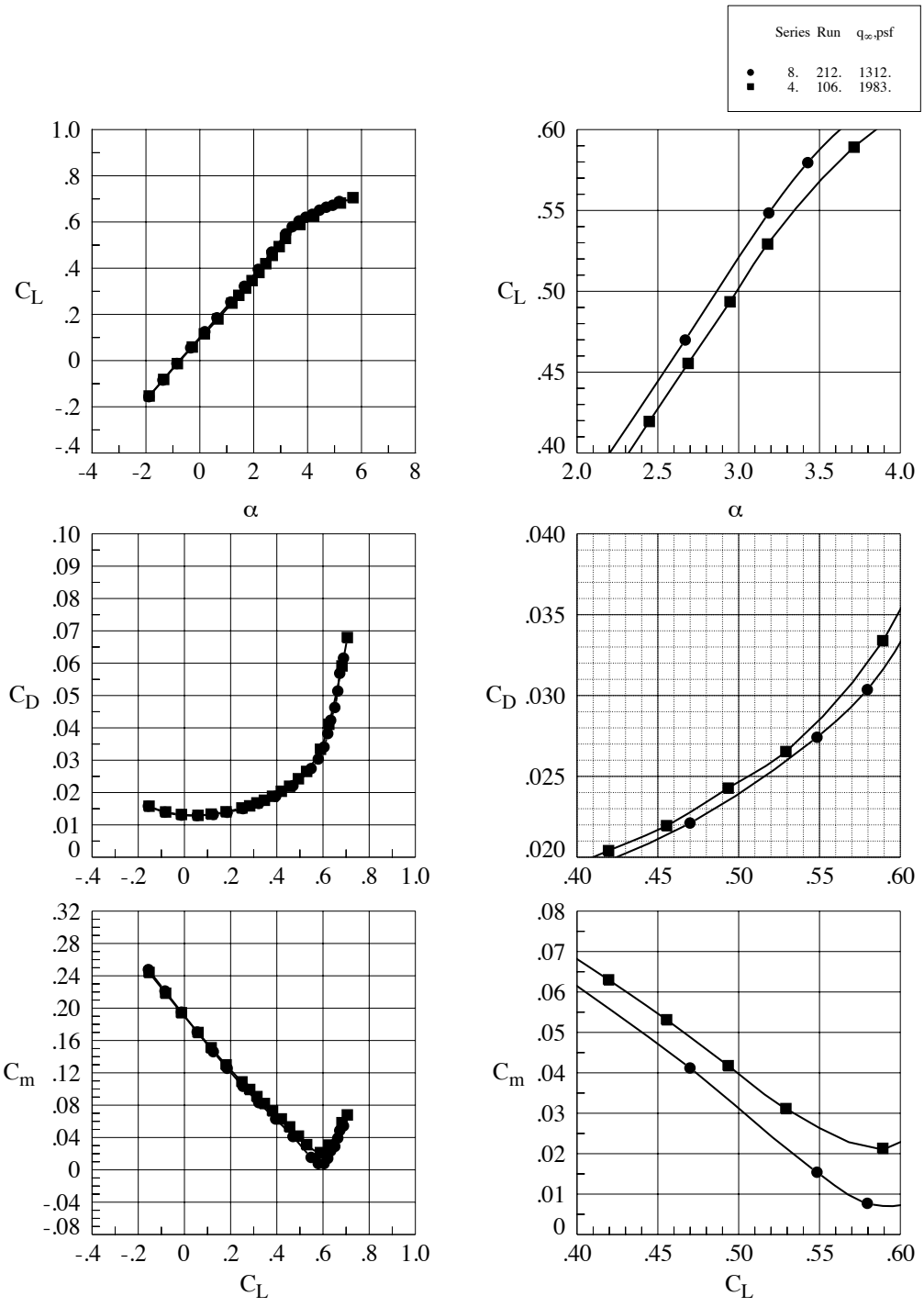

Fig. 9. NTF 197, aeroelastic effects, WBT0, M_∞ = 0.85, Re_c = 19.8 million.

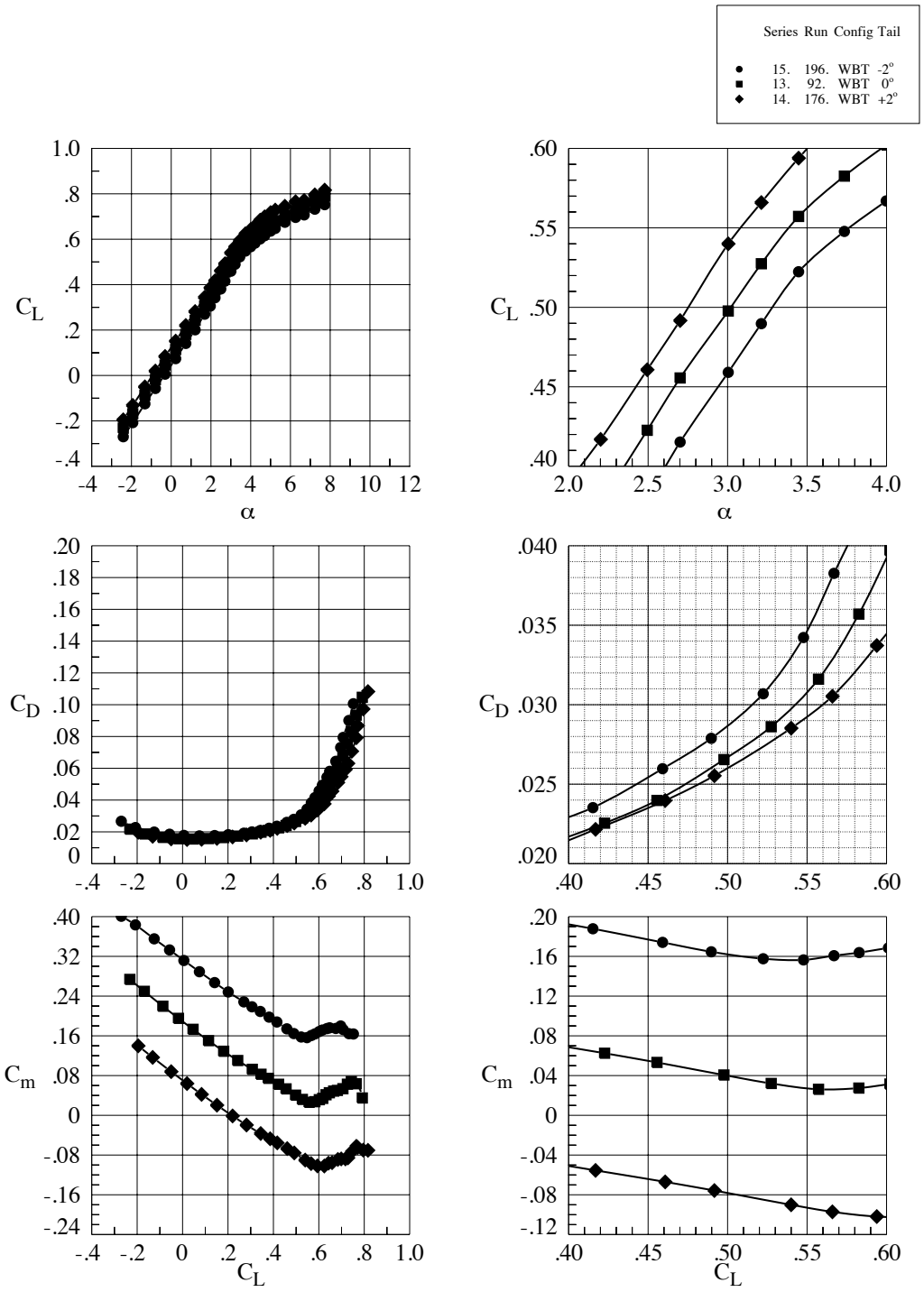

Fig. 10. NTF 197, tail effects, $M_\infty = 0.85$, $Re_c = 5$ million.

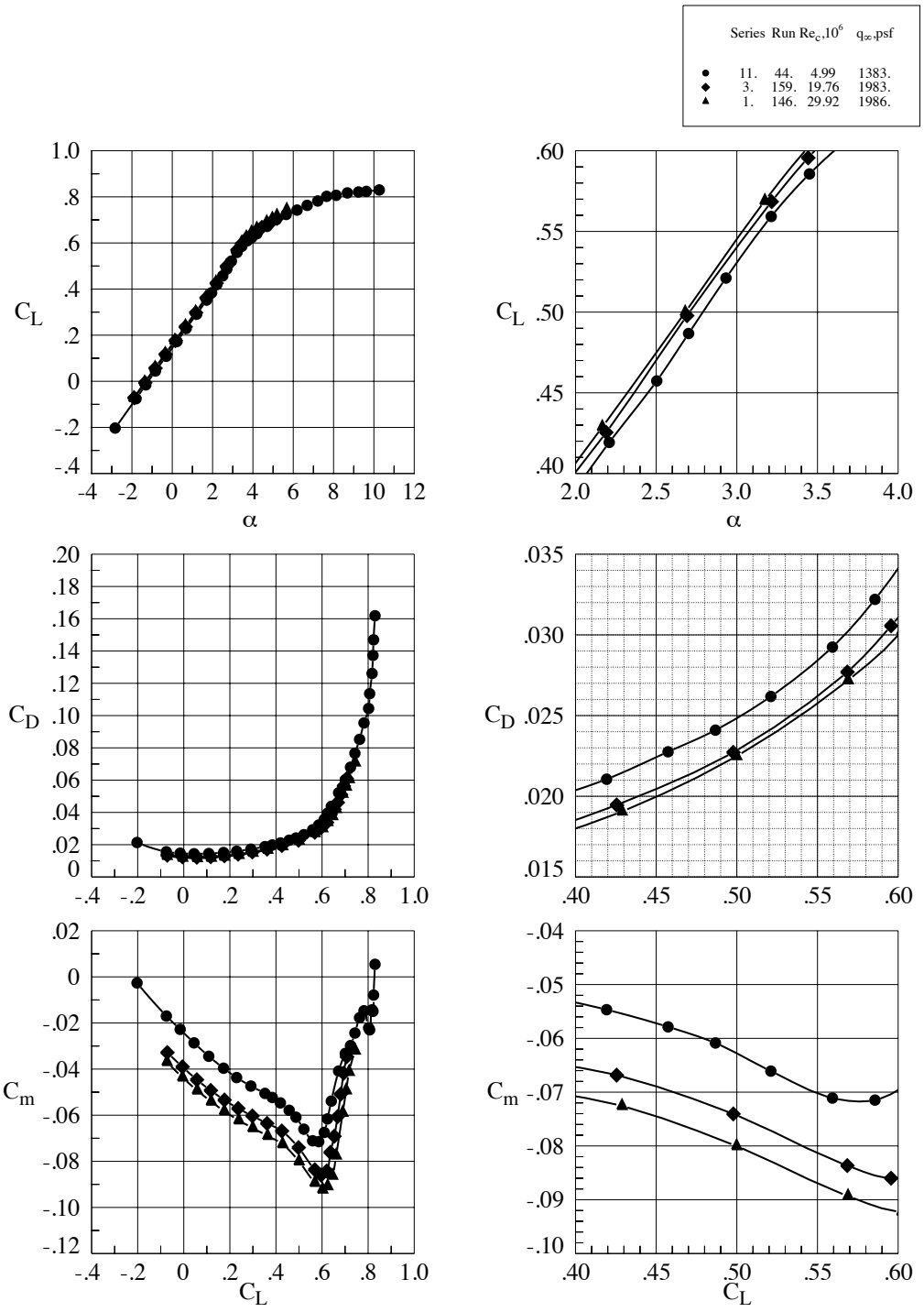

Fig. 11. NTF 197, Reynolds number effects, WB, M_∞ = 0.85.

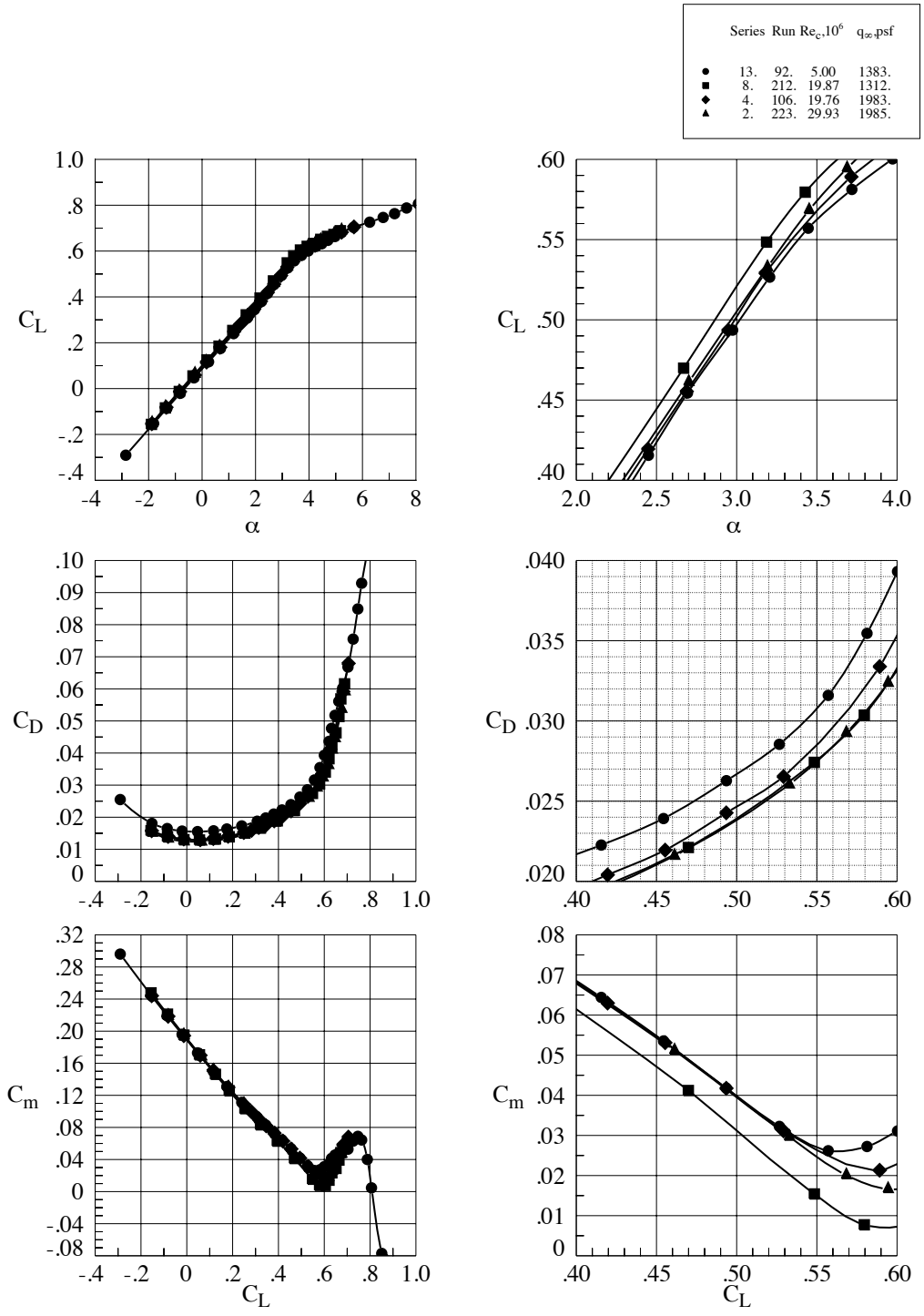

Fig. 12. NTF 197, Reynolds number effects, WBT0, M_∞ = 0.85.

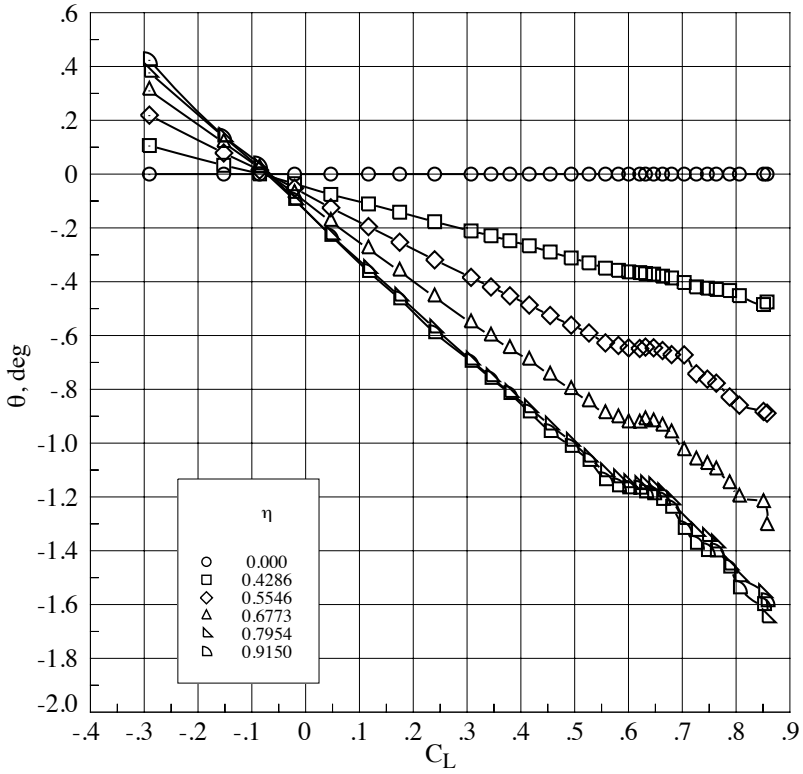

Fig. 13. NTF 197, wing twist, WBT0, M_∞ = 0.85, Re_c = 5 million.

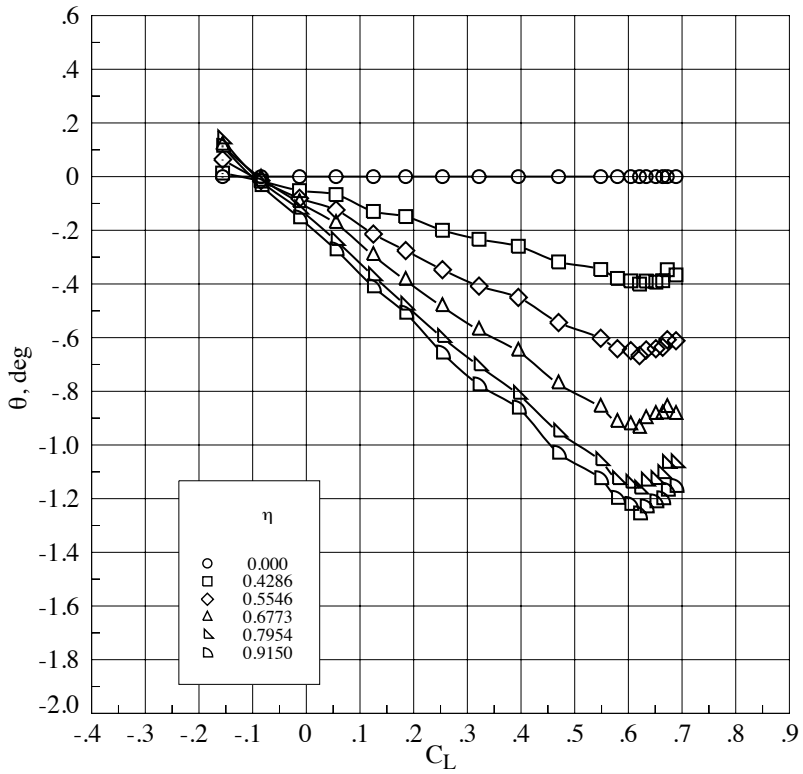

Fig. 14. NTF 197, wing twist, WBT0, M_∞ = 0.85, Re_c = 19.8 million, low q_∞.

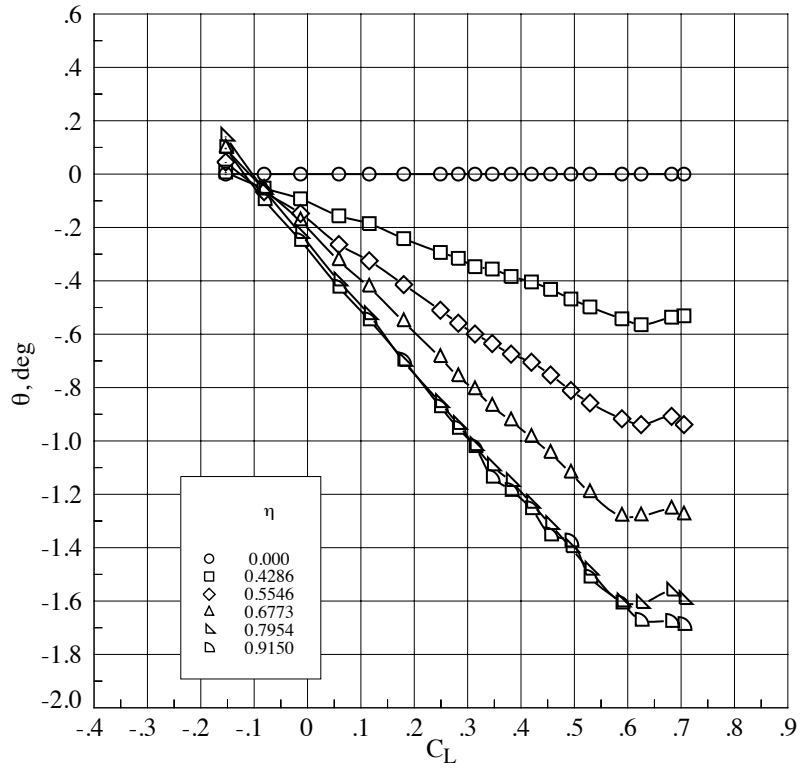

Fig. 15. NTF 197, wing twist, WBT0, M_∞ = 0.85, Re_c = 19.8 million, high q_∞.

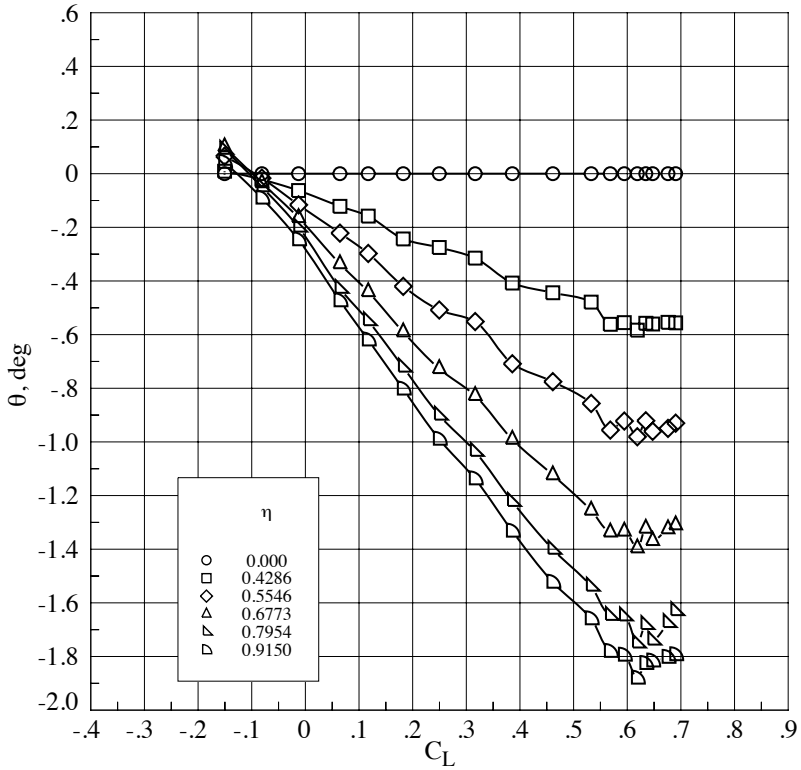

Fig. 16. NTF 197, wing twist, WBT0, M_∞ = 0.85, Re_c = 30 million.

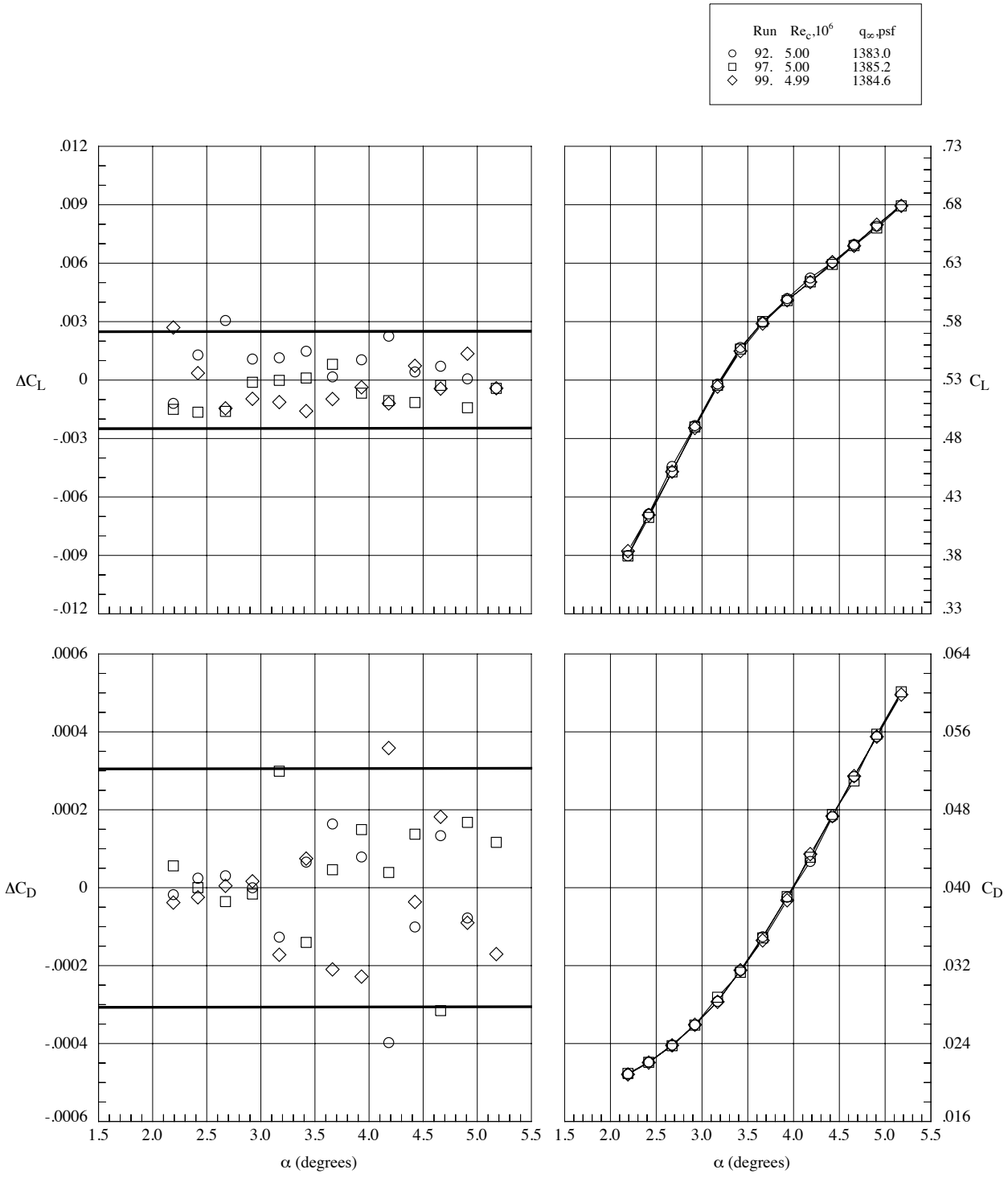

Fig. 17. NTF 197 data repeatability, WBT0 configuration, $M_\infty = 0.85$, $Re_c = 5x10^6$. Solid line indicates 2-sigma limits based on the residual data.

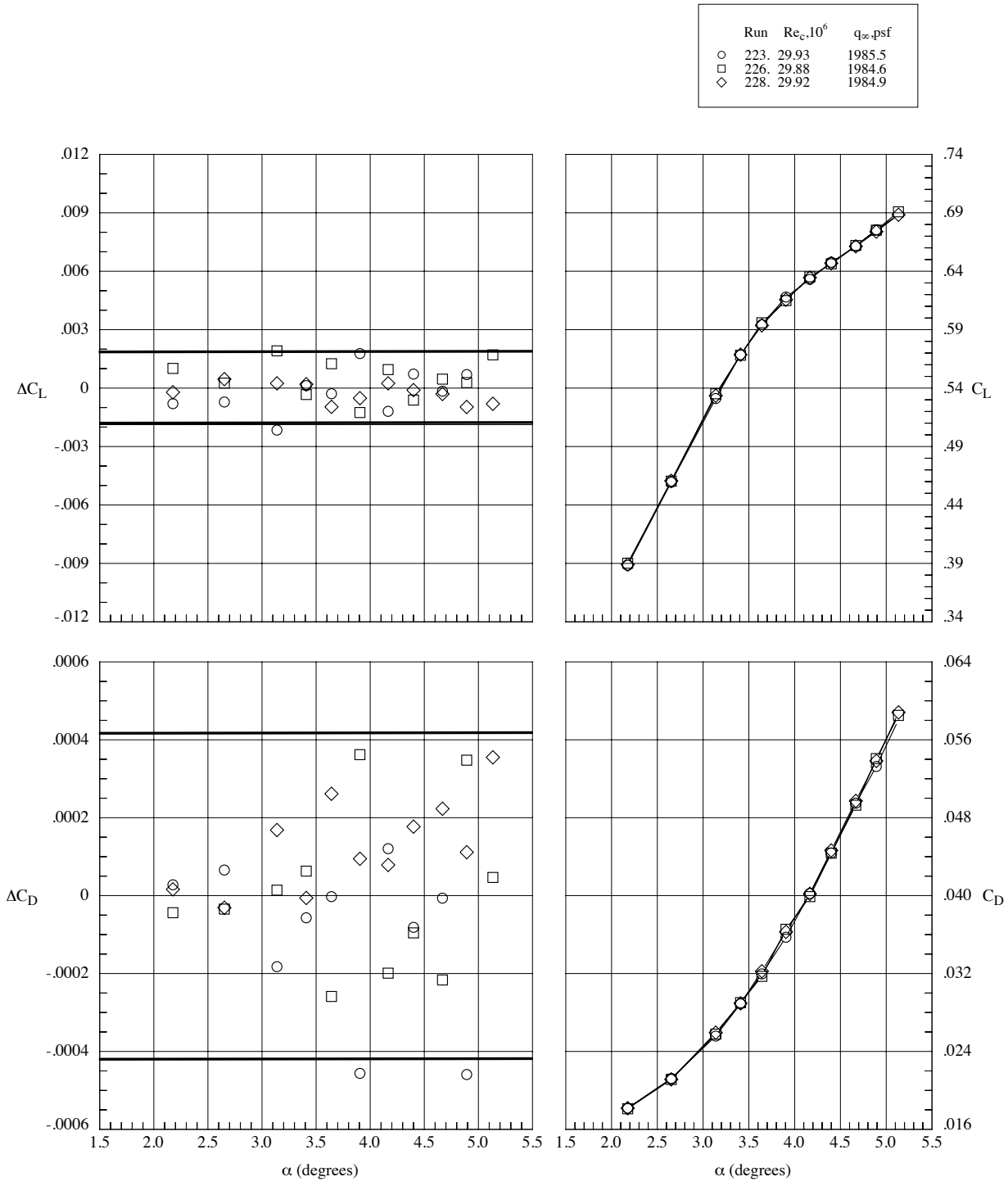

Fig. 18. NTF 197 data repeatability, WBT0 configuration, $M_\infty = 0.85$, $Re_c = 30x10^6$. Solid line indicates 2-sigma limits based on the residual data.

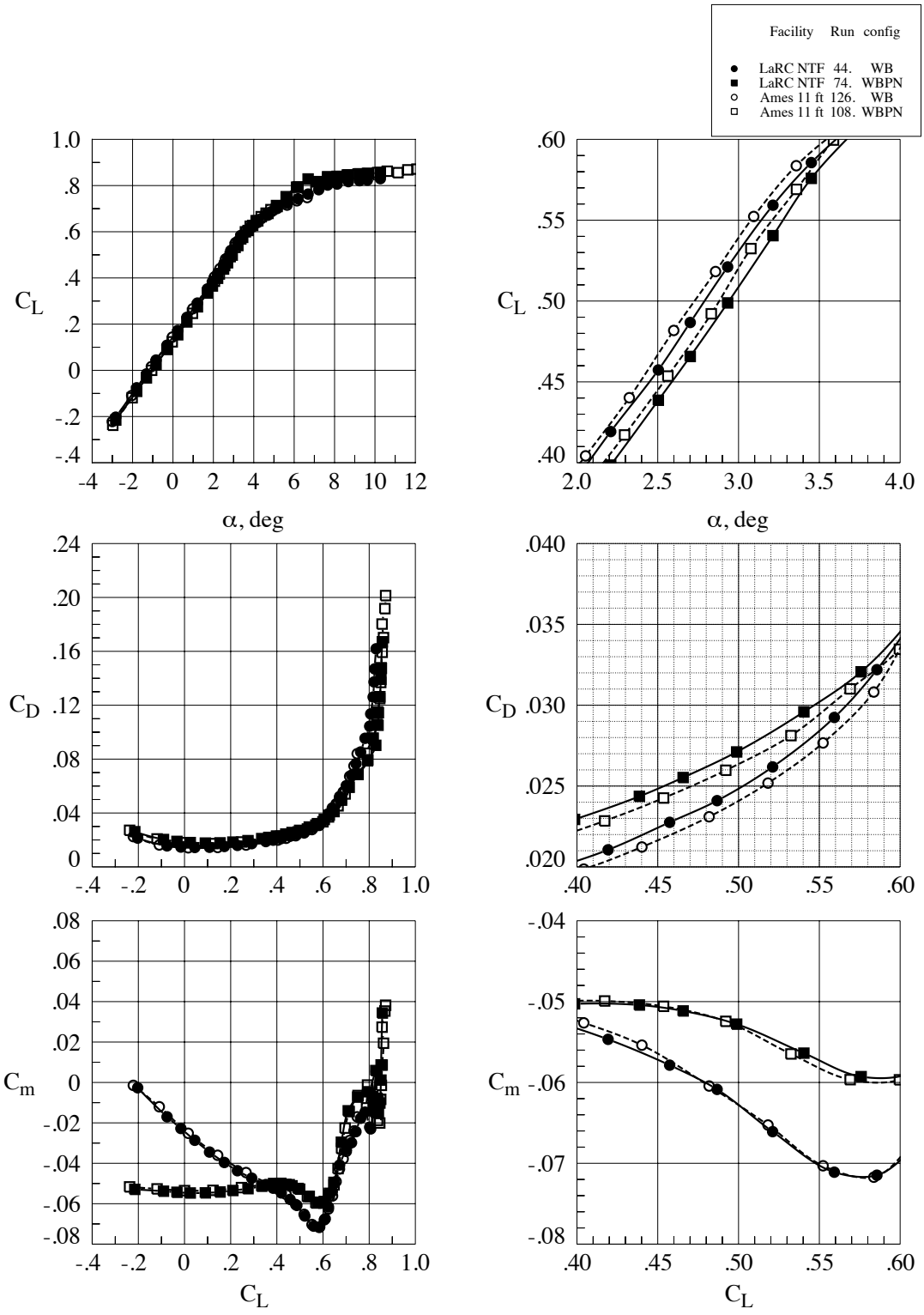

Fig. 19. NTF 197 and Ames 11-ft, nacelle/pylon effects, $M_\infty = 0.85$, $Re_c = 5x10^6$.

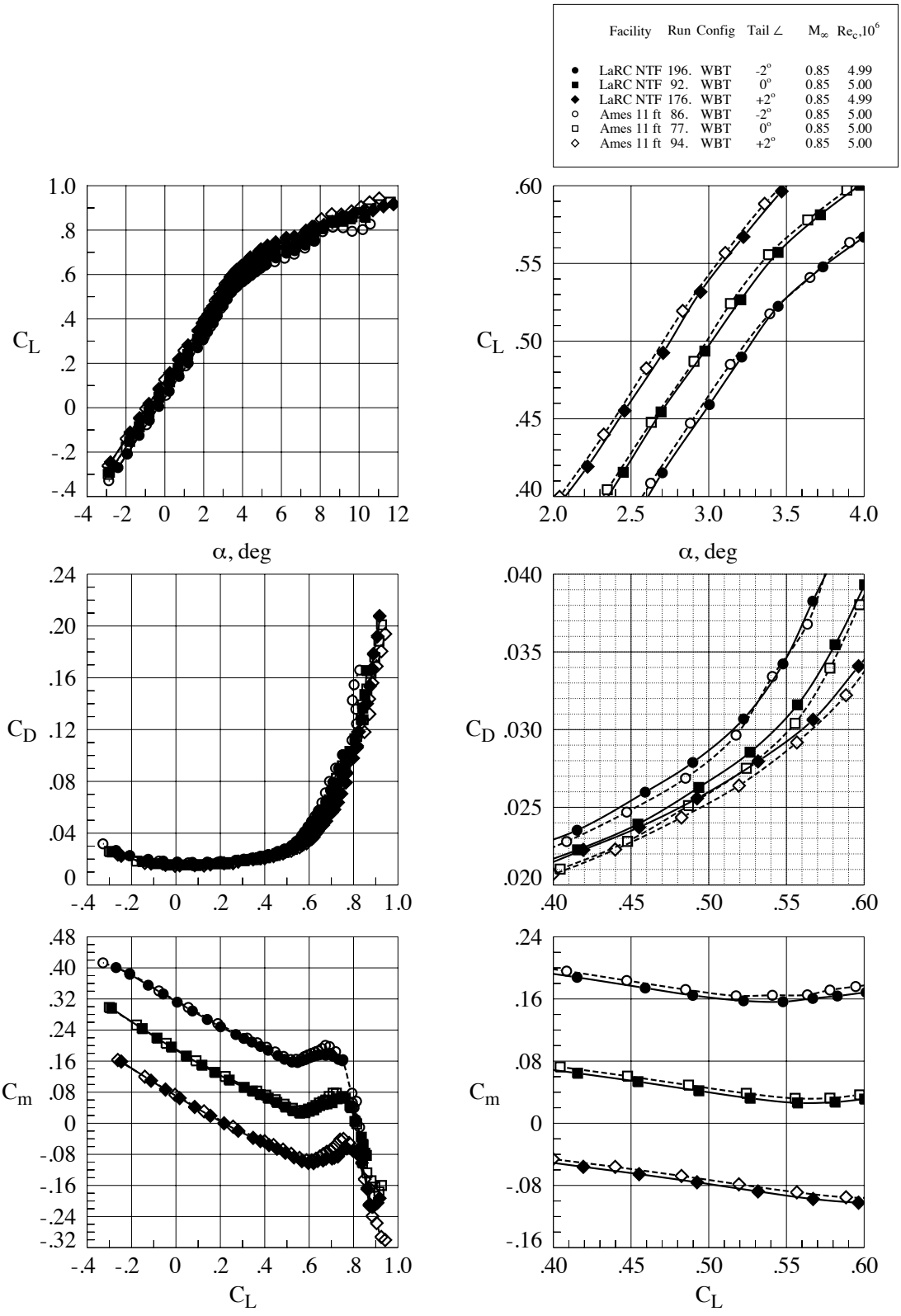

Fig. 20. NTF 197 and Ames 11-ft, tail effects, $M_\infty = 0.85$, $Re_c = 5x10^6$.

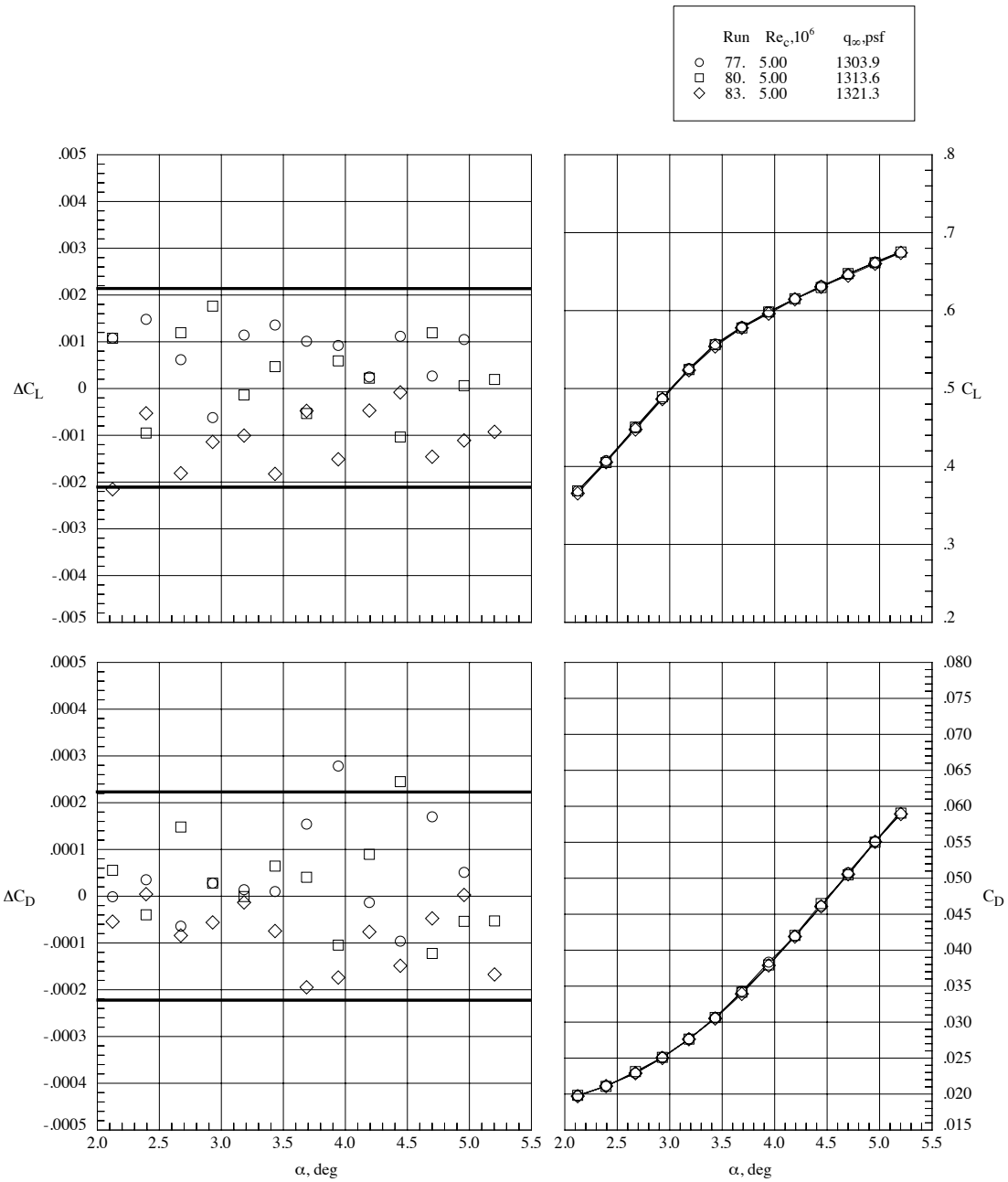

Fig. 21. Ames 11-ft data repeatability, WBT0 configuration, $M_\infty = 0.85$, $Re_c = 5x10^6$. Solid line indicates 2-sigma limits based on the residual data.

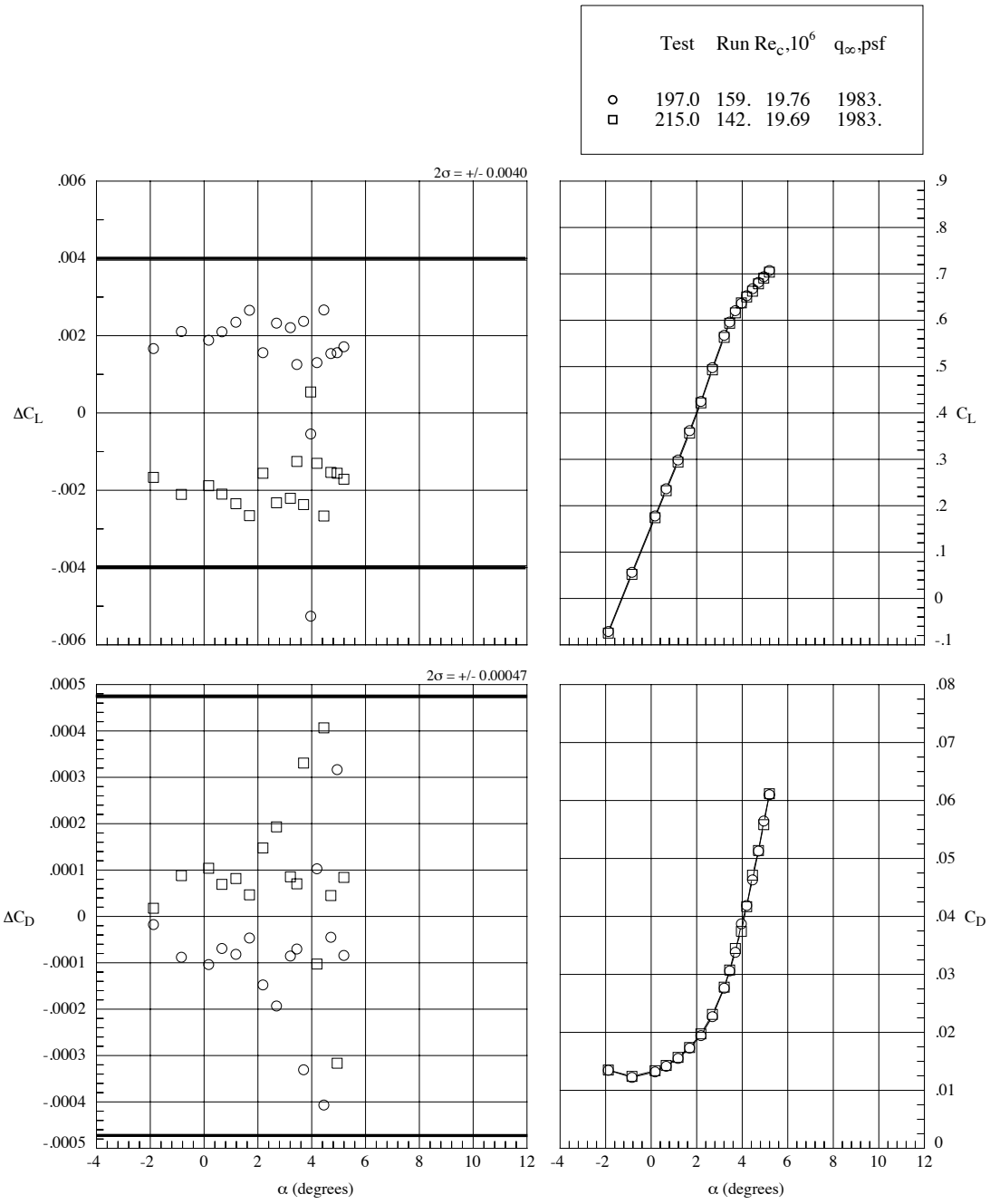

Fig. 22. NTF test to test repeatability, WB, M_∞ = 0.85, Re_c = 19.8 million. Solid line indicates 2-sigma limits based on the residual data.

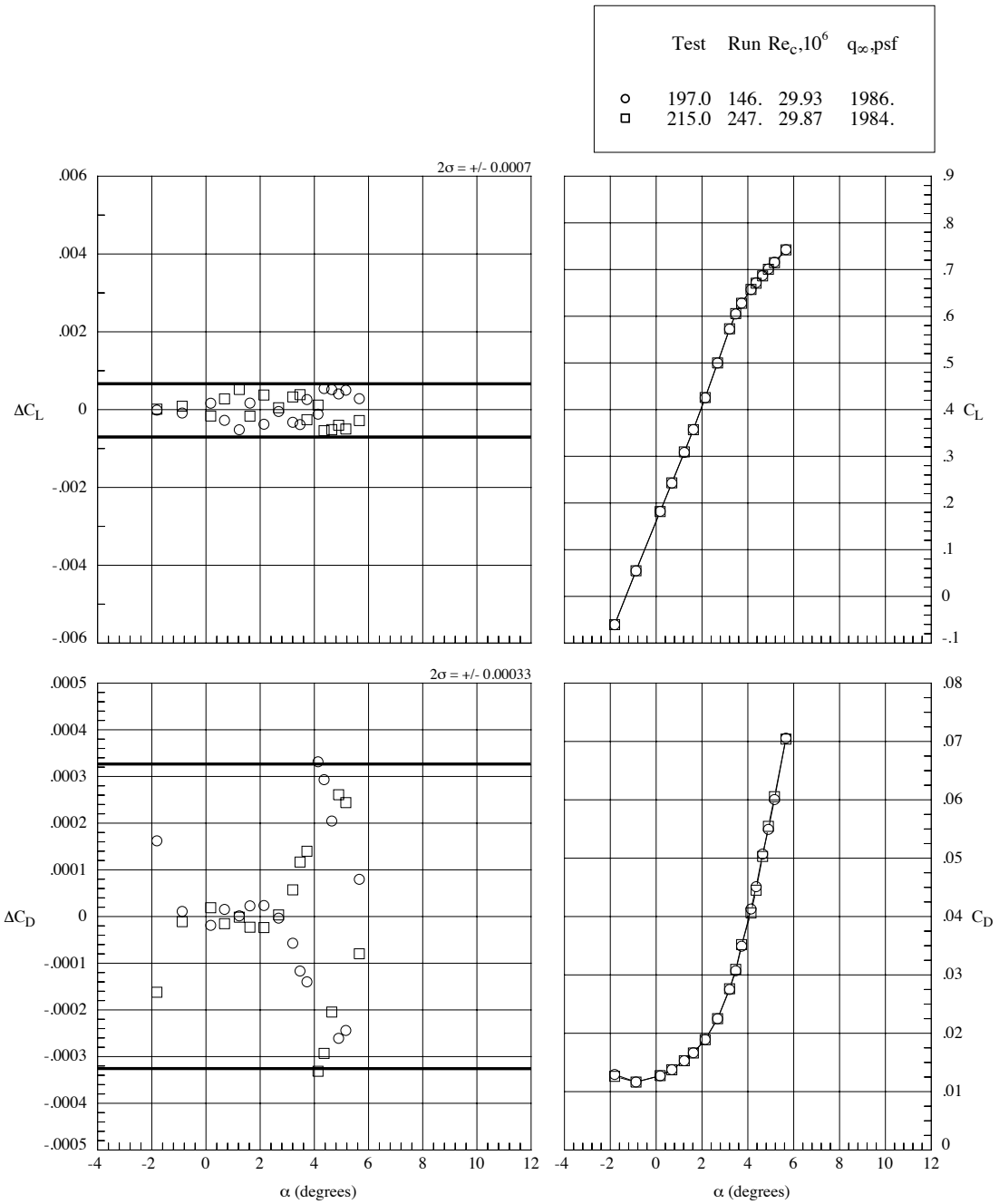

Fig. 23. NTF test to test repeatability, WB, M_∞ = 0.85, Re_c = 30 million. Solid line indicates 2-sigma limits based on the residual data.

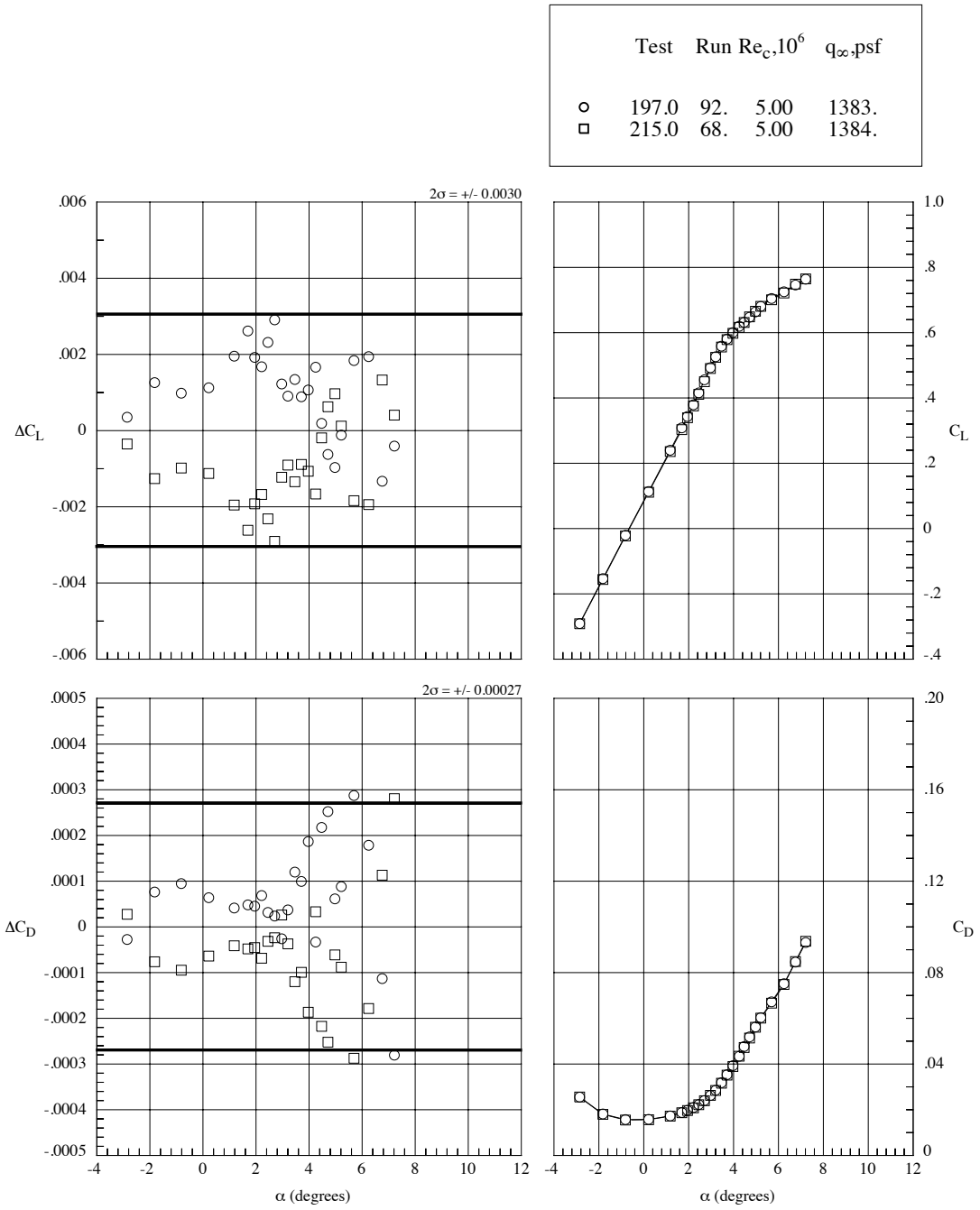

Fig. 24. NTF test to test repeatability, WBT0, M_∞ = 0.85, Re_c = 5 million. Solid line indicates 2-sigma limits based on the residual data.

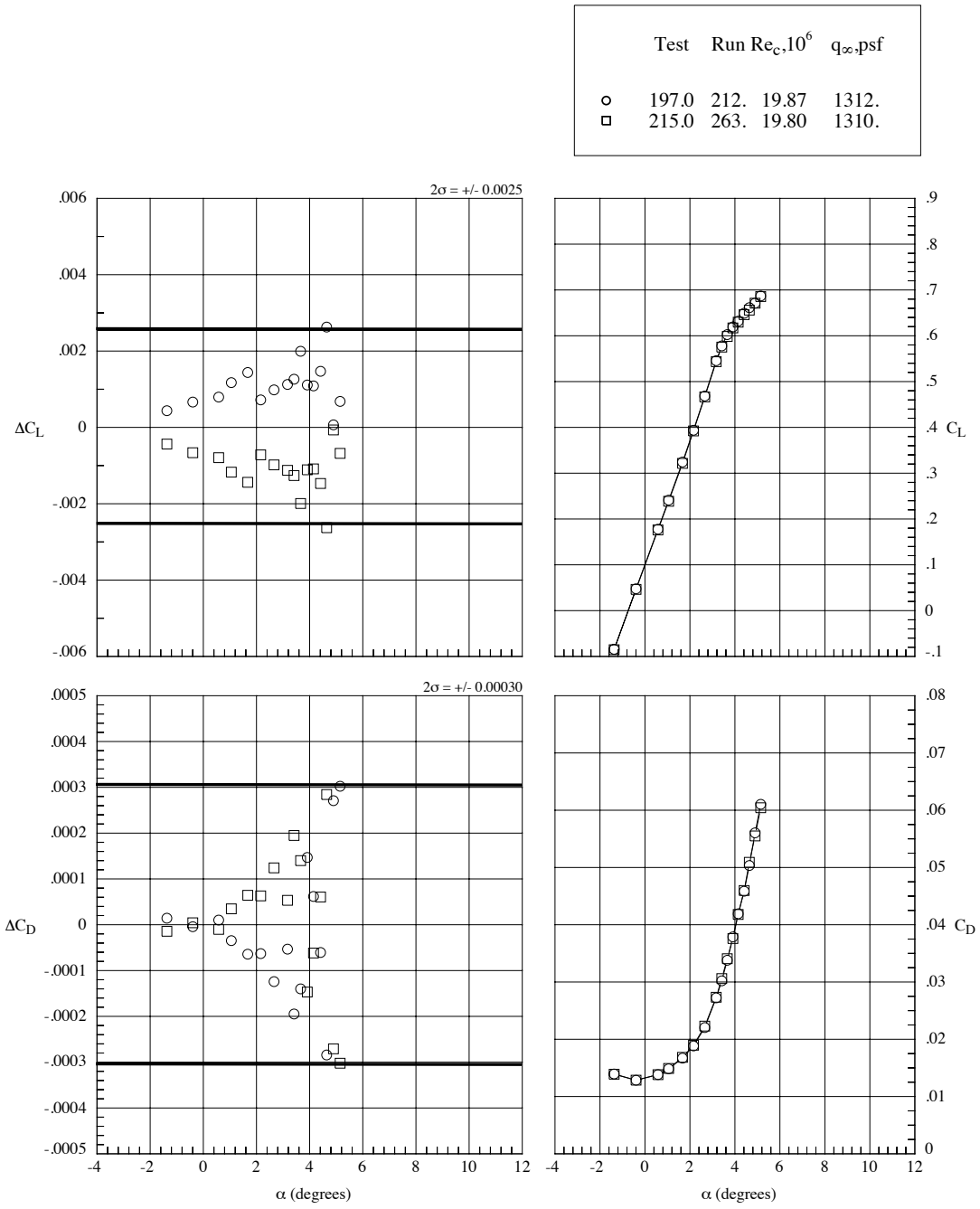

Fig. 25. NTF test to test repeatability, WBT0, M_∞ = 0.85, Re_c = 19.8 million, low q_∞. Solid line indicates 2-sigma limits based on the residual data.

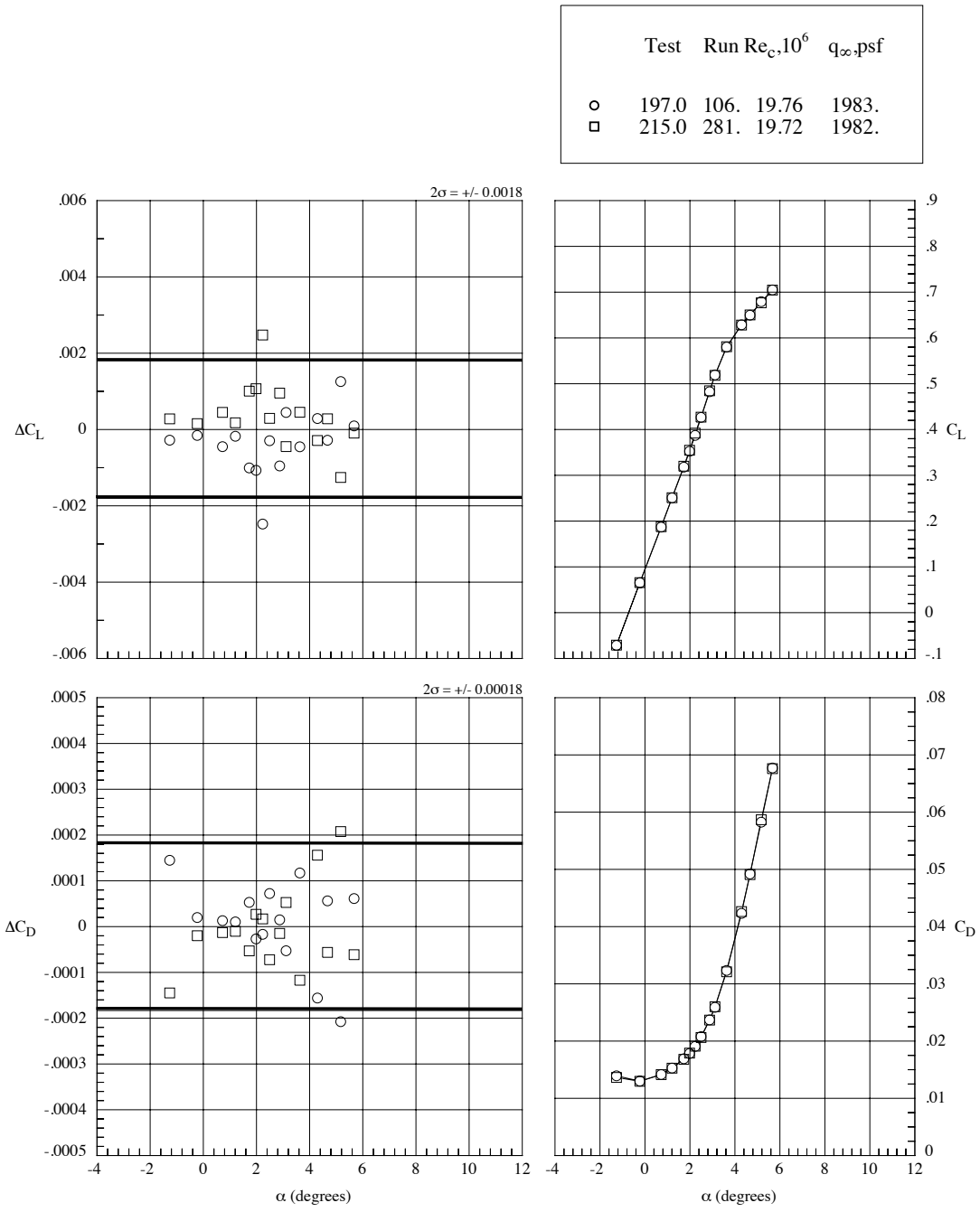

Fig. 26. NTF test to test repeatability, WBT0, M_∞ = 0.85, Re_c = 19.8 million, high q_∞. Solid line indicates 2-sigma limits based on the residual data.

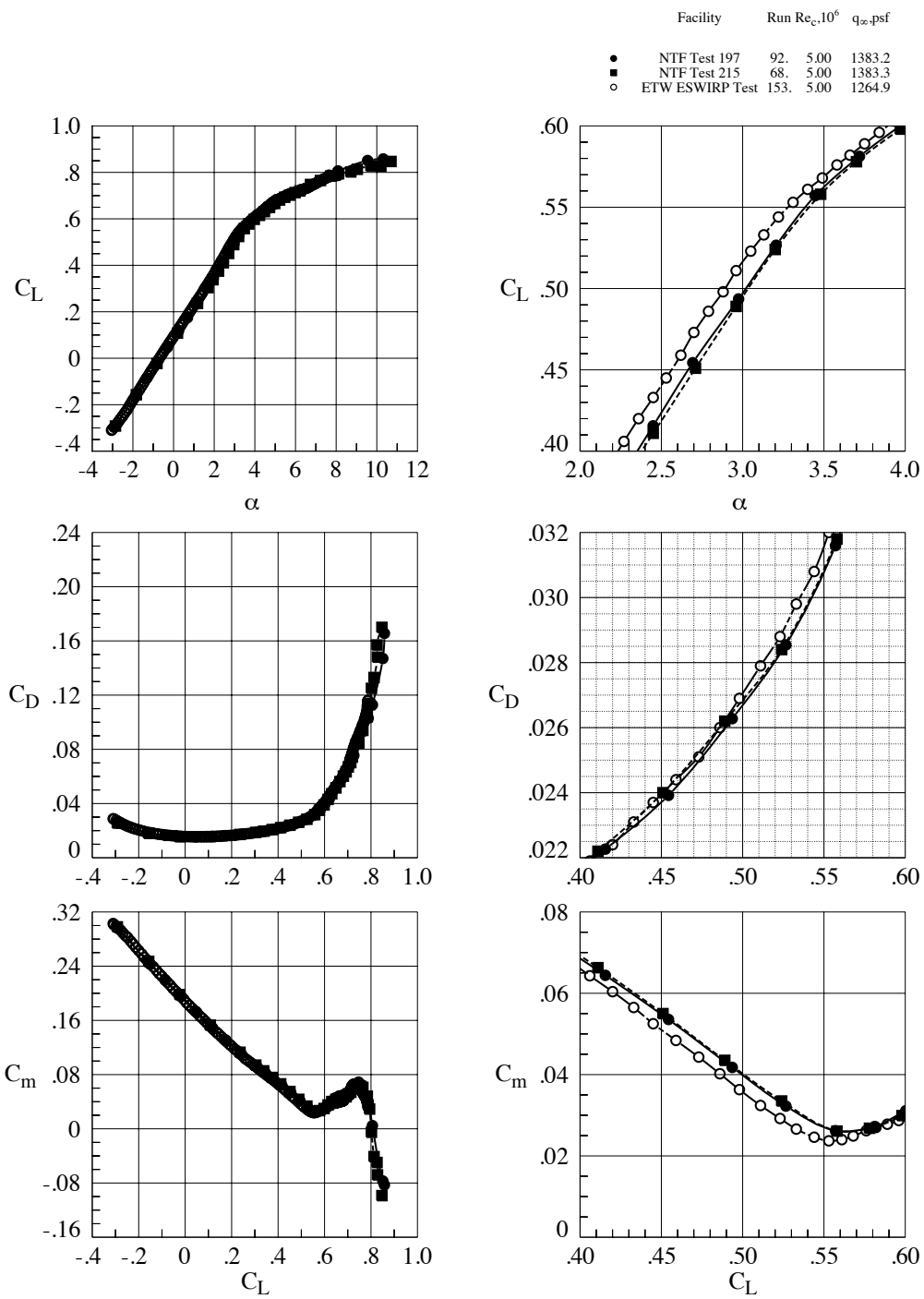

Fig. 27. NTF and ETW test to test comparison, $M_\infty = 0.85$, $Re_c = 5x10^6$.

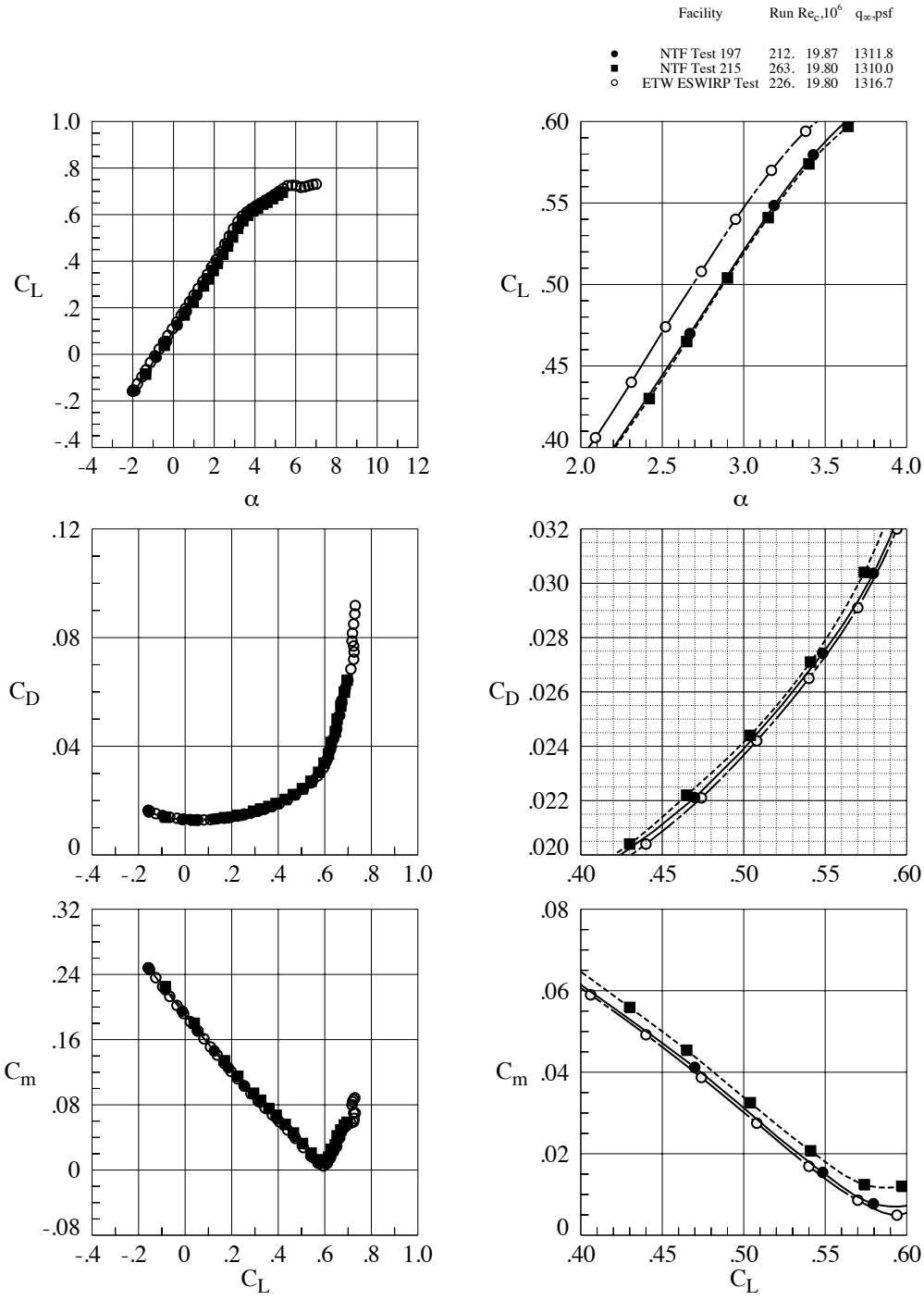

Fig. 28. NTF and ETW test to test comparison, M_∞ = 0.85, Re_c = 19.8x10^6, low q_∞.

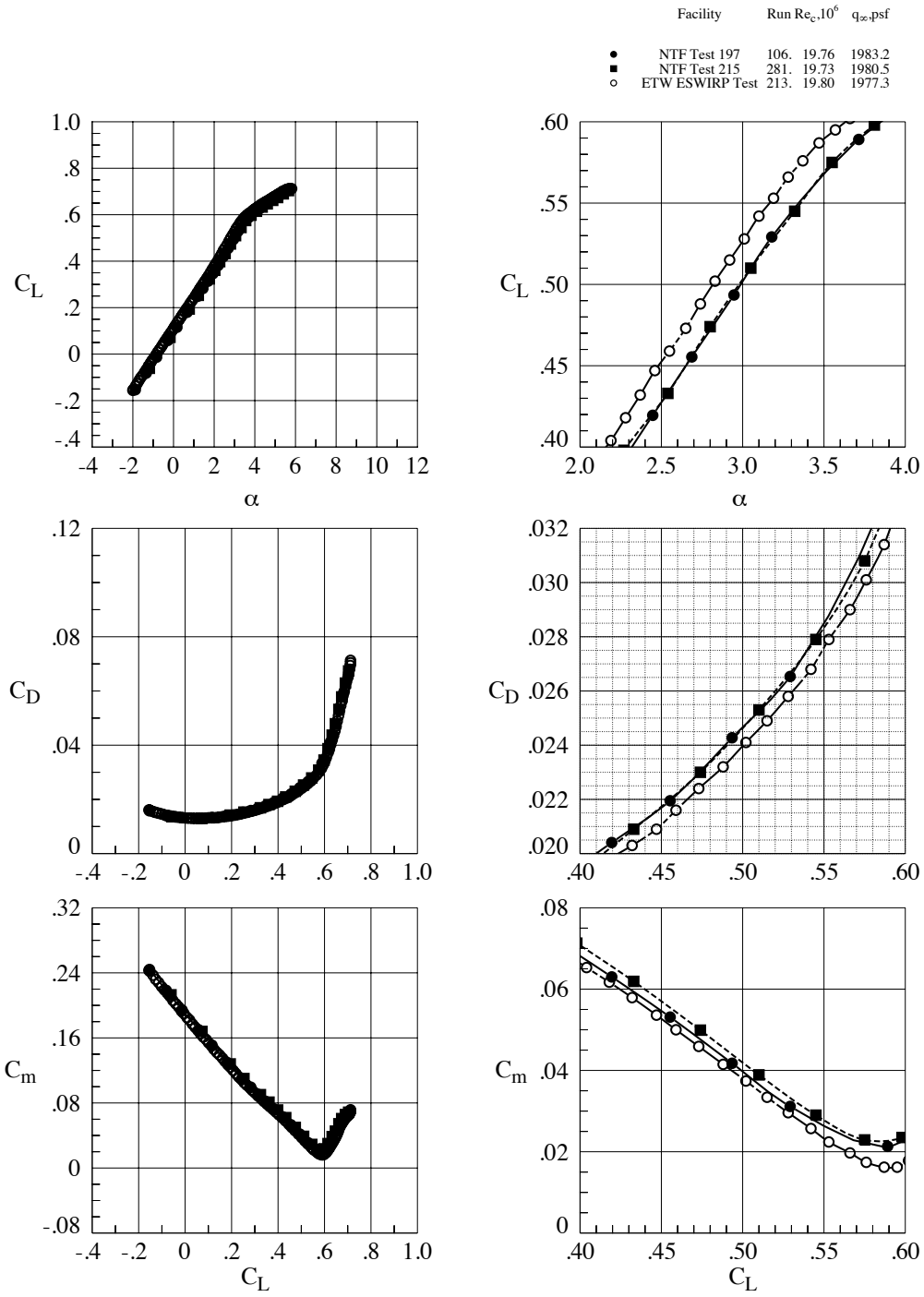

Fig. 29. NTF and ETW test to test comparison, $M_\infty = 0.85$, $Re_c = 19.8x10^6$, high q_∞.

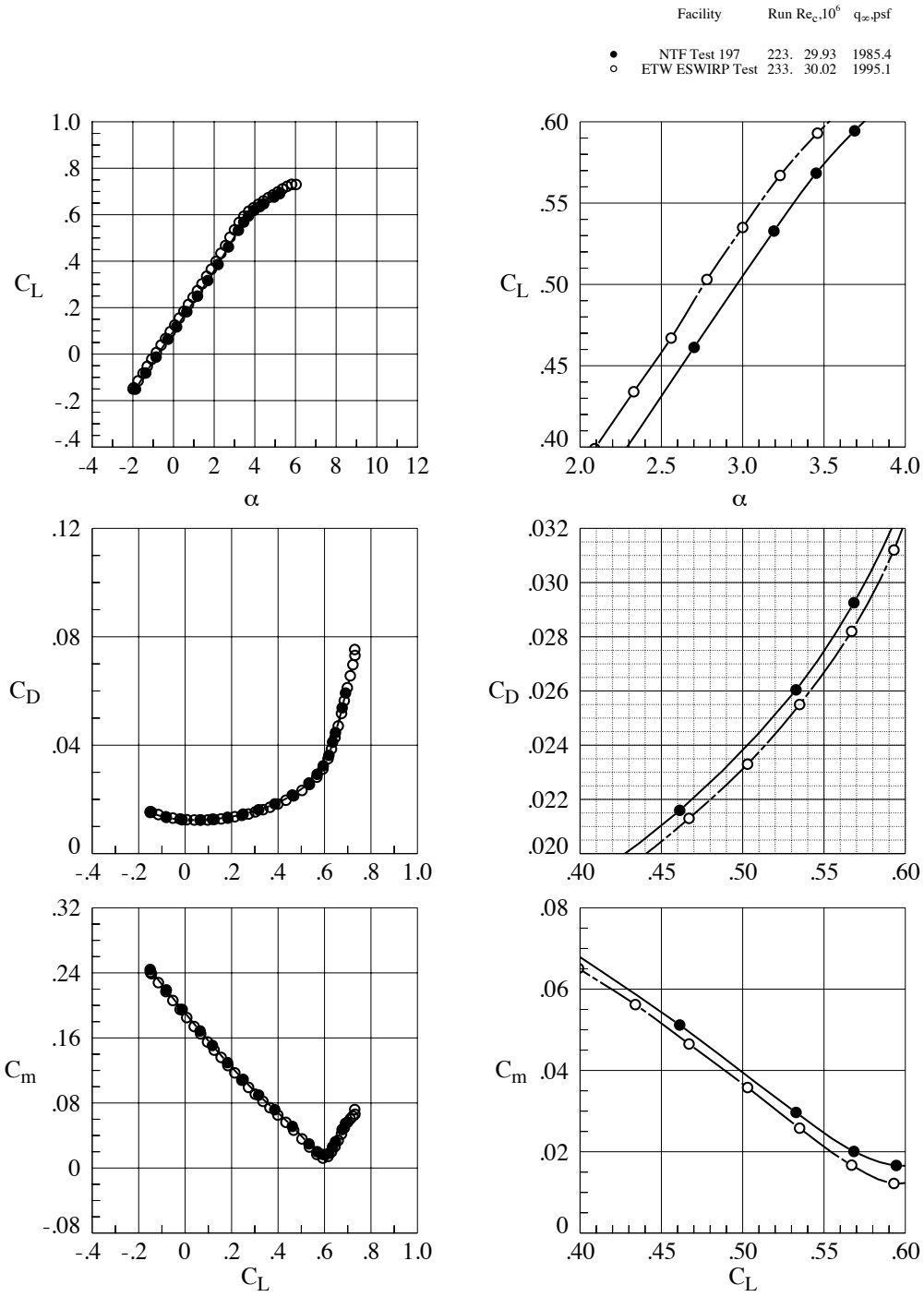

Fig. 30. NTF and ETW test to test comparison, $M_\infty = 0.85$, $Re_c = 30x10^6$.

Fig. 31. The 80% scaled CRM model installed in the JAXA 2m x 2m Transonic Wind Tunnel.

Fig. 32. The ONERA Large Reference Model installed in the ONERA S1MA wind tunnel.

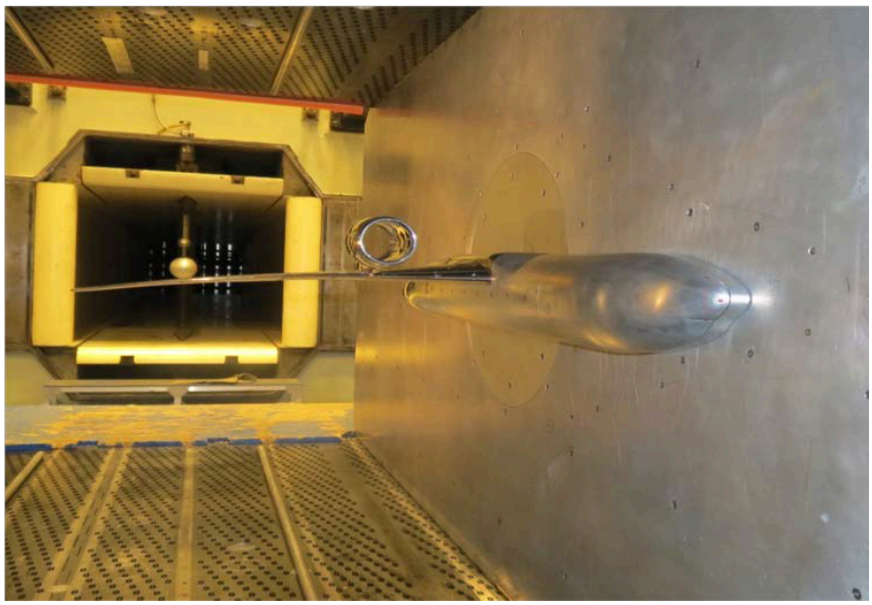

Fig. 33. CRM semispan model installed inverted in the NRC 5-Foot wind tunnel.

Fig. 34. Photo of the CRM-HL model installed in the 14- by 22-Foot Subsonic Wind Tunnel at the NASA Langley Research Center.

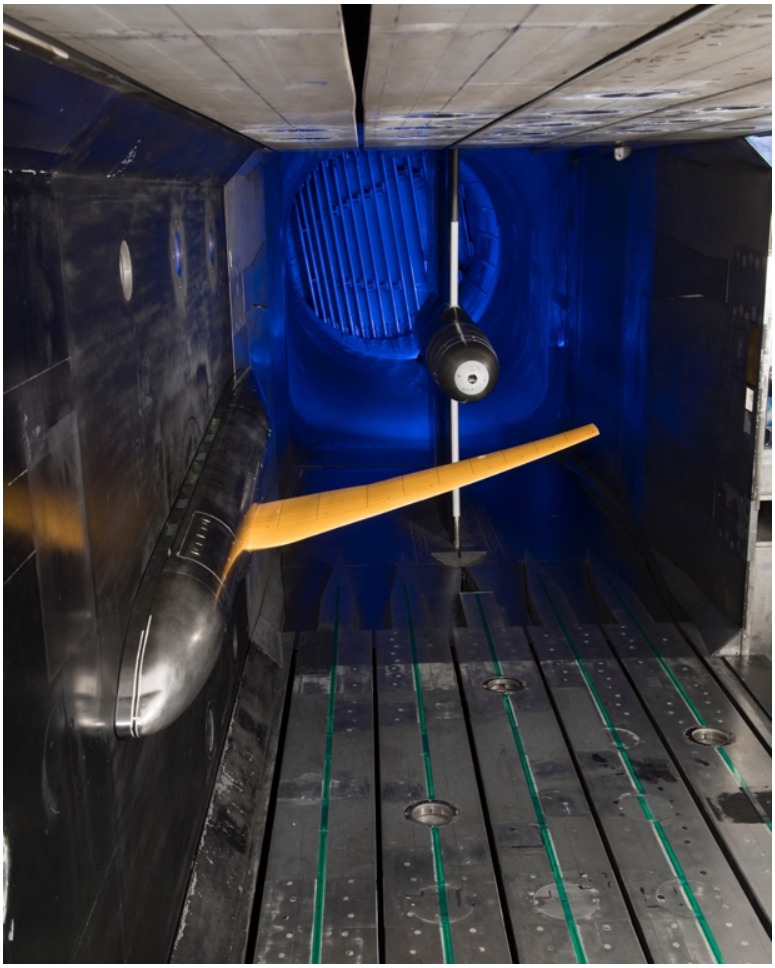

Fig. 35. Photo of the Common Research Model with Natural Laminar Flow wing in the National Transonic Facility.